

Quantum Extremal Modular Curvature: Modular Transport with Islands

Lars Aalsma^{a,b}, Cynthia Keeler^b, Claire Zukowski^c,

^a*Beyond: Center for Fundamental Concepts in Science, Arizona State University, Tempe, Arizona 85287, USA*

^b*Department of Physics, Arizona State University, Tempe, Arizona 85287, USA*

^c*Department of Physics and Astronomy, University of Minnesota Duluth, Duluth, MN 55812, USA*

laalsma@asu.edu, keelerc@asu.edu, czukowsk@d.umn.edu

ABSTRACT: Modular Berry transport is a useful way to understand how geometric bulk information is encoded in the boundary CFT: The modular curvature is directly related to the bulk Riemann curvature. We extend this approach by studying modular transport in the presence of a non-trivial quantum extremal surface. Focusing on JT gravity on an AdS background coupled to a non-gravitating bath, we compute the modular curvature of an interval in the bath in the presence of an island: the Quantum Extremal Modular Curvature (QEMC). We highlight some important properties of the QEMC, most importantly that it is non-local in general. In an OPE limit, the QEMC becomes local and probes the bulk Riemann curvature in regions with an island. Our work gives a new approach to probe physics behind horizons.

Contents

1	Introduction	1
2	Modular Transport and Berry Curvature	3
2.1	Introduction to Modular Transport	4
2.2	Modular Transport in Holography	6
3	Modular Transport in JT Gravity	13
3.1	JT Gravity on AdS ₂	13
3.2	Modular Transport for a Single Interval	18
3.3	Modular Transport in the Presence of an Island	22
4	Discussion	32
A	Riemann Curvature from Fermi Normal Coordinates	34
A.1	General Procedure	34
A.2	Example: Diagonal Geodesic in AdS ₃	35
B	Generators of Modular Transport	37
B.1	Generators in x -space	37
B.2	Generators in X -space	38

1 Introduction

In the context of the AdS/CFT correspondence, entanglement entropy has provided key insights as to how geometry emerges from conformal field theories. The Ryu-Takayanagi (RT) formula [1] (and its covariant generalization [2]) has played an essential role in these developments as it relates CFT entanglement entropy to the area of bulk minimal surfaces. Of course, the RT formula is just one example that demonstrates how some piece of geometric information is encoded in the CFT. A promising approach towards understanding how more general geometric properties emerge from holographic CFTs is modular transport.

This method, pioneered in [3, 4] and inspired by related work on kinematic space [5–8], defines a parallel transport problem for modular Hamiltonians that are deformed

by changing CFT subregions (see also [9, 10] for other approaches to Berry transport in holography, and [11–13] for other methods for reconstructing the bulk geometry). The transport process admits a redundancy in the form of zero modes that commute with the modular Hamiltonian. This redundancy is analogous to the Berry phase in quantum mechanics and was therefore referred to as a modular Berry phase. By gauging this redundancy one finds a modular curvature, again analogous to the well-known Berry curvature. One key result of [4] was to show how—in holography—geometry is encoded in the modular curvature. In many cases of interest, the action of the modular Hamiltonian reduces to a boost isometry near the edge of the entanglement wedge. Exploiting this relation, it was demonstrated that the modular curvature is related to the Riemann tensor [4, 14].

Subsequent work not only considered changes in the modular Hamiltonian due to changing CFT subregions (known as shape deformations), but also changes due to modifying the state (referred to as state deformations) [15, 16]. The references [15, 16] showed that the modular curvature associated to state deformations is related to a bulk symplectic form. What these different examples have in common is that the modular curvature probes some piece of interesting bulk geometric information.

When considering a subregion in the CFT, we only have access to the portion of the bulk covered by the entanglement wedge [17]. So-called “entanglement shadow regions” were shown to be impenetrable by boundary-anchored minimal surfaces [18, 19], while surfaces of nonpositive extrinsic curvature dubbed “barriers” were shown to obstruct boundary-anchored extremal surfaces in the covariant description [20]. Since the modular transport approach to bulk reconstruction uses bulk extremal surfaces to probe the Riemann curvature, it has the seeming drawback that barriers may prevent reconstruction in arbitrary bulk regions, for instance deep inside a black hole.

One motivation of this work is to see how this obstruction can be partly overcome by making use of quantum extremal surfaces (QESs) [21]. Studies on the black hole information paradox revealed that the entanglement wedge of black hole radiation can include an ‘island’ QES region that is disconnected from the boundary and can lie behind the horizon [22, 23]. In this paper, we therefore focus on modular transport in the presence of an island which involves performing modular flow on two disjoint subregions. We are interested in understanding if and what geometrical information about the bulk is encoded in the modular curvature in the presence of a non-trivial QES: a quantity which we refer to as the ‘Quantum Extremal Modular Curvature’ (QEMC).

We focus on a 1 + 1-dimensional free fermion theory coupled to JT gravity, since there is a closed-form expression for its modular Hamiltonian for n disjoint subregions [24]. The modular Hamiltonian of the free fermion was used in the context of islands

in [25], and its modular curvature on flat space backgrounds has been studied in [26]. Our contribution is to put these results to work in our setup of interest, which is JT gravity on an AdS_2 background coupled to a non-gravitating bath region. The free fermion theory lives on this background and allows us to analytically study modular transport in the presence of islands.

Our setup is somewhat different than the one considered in previous studies of modular transport in holography. Typically, a subregion in the CFT_d is used to define bulk entanglement wedges in AdS_{d+1} : modular flow in the CFT_d has a direct analog in AdS_{d+1} . However, the dual of JT gravity coupled to a non-gravitational bath is a quantum mechanical (QM) theory. Instead of defining subregions in this QM theory we work directly in the semi-classical ‘gravitational picture’ and define a subregion in the two-dimensional non-gravitational bath which, via the QES condition, also identifies a subregion in the bulk. This is the same as the setup for computing the entanglement entropy of Hawking radiation in the presence of islands.

A main result of our paper is that—in an OPE limit—the QEMC still probes bulk Riemann curvature including near the island region. This yields a method to access geometrical information, possibly behind a horizon, from the non-gravitational bath region. Away from this simplifying limit, the curvature contains non-local terms that have their origin in the non-local nature of the modular Hamiltonian for disjoint intervals. It is tempting to speculate that these non-local corrections signal some sort of breakdown of the semi-classical EFT along the lines of [27, 28], but we leave further interpretation to future work.

The rest of this paper is organized as follows. In Sec. 2, we review the process of modular transport and explain how it probes bulk Riemann curvature. As a concrete and illustrative example we focus on $\text{AdS}_3/\text{CFT}_2$, generalizing some of the results in [15, 16]. In Sec. 3, we focus on JT gravity and consider a solution that contains a non-trivial quantum extremal surface. We then introduce modular flow in this background and compute various components of the QEMC. We end with a discussion of our results in Sec. 4.

2 Modular Transport and Berry Curvature

We start with a short review of modular Hamiltonians and the transport process that probes the bulk geometry.

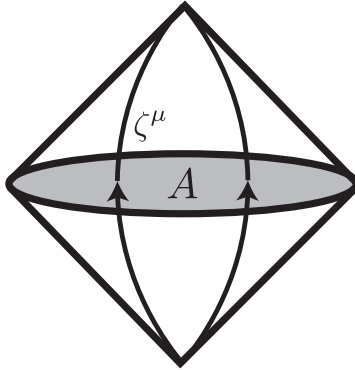


Figure 1. Causal diamond associated to the subregion A . The vector field ζ^μ is a boost vector that preserves the diamond.

2.1 Introduction to Modular Transport

Given a quantum state $|\psi\rangle$ and a spatial subregion A the reduced density matrix is defined as

$$\rho_A = \text{tr}_{\bar{A}} |\psi\rangle \langle \psi| , \quad (2.1)$$

where we perform a trace over \bar{A} , the complement of A . The formal definition of the modular Hamiltonian H of this subregion is

$$H = -\ln \rho_A . \quad (2.2)$$

Using s to denote the modular ‘time’ parameter, the evolution of an operator under modular flow is given by

$$\mathcal{O}(s) \rightarrow \mathcal{O}(s') = e^{\frac{i(s'-s)}{2\pi} H} \mathcal{O}(s) e^{-\frac{i(s'-s)}{2\pi} H} . \quad (2.3)$$

For general states and subregions, the modular Hamiltonian is a complicated and possibly non-local operator. However, in certain special cases such as a single interval in the Minkowski vacuum [29], it obeys the local expression

$$H = \int_A d\Sigma \zeta^\mu n^\nu T_{\mu\nu} . \quad (2.4)$$

Here ζ^μ is the boost vector that preserves the causal diamond defined by the subregion A (see Figure 1), n^μ is the unit normal to A , and $T_{\mu\nu}$ is the stress tensor.

As explained in [30], locality of the modular Hamiltonian is directly related to ultralocality of correlation functions, in the vacuum. More generally, for states that are perturbations away from the vacuum, the modular Hamiltonian acts as a local

boost close to the horizons of the diamond [31]. Intuitively, excited states like those considered in [31] look like the vacuum at short distances. For multiple subregions in the vacuum, the modular Hamiltonian again is non-local.

When changing the subregion or the state, the modular Hamiltonian also changes. As studied in depth in [4, 14–16], we can define a modular transport problem by parallel transporting the modular Hamiltonian. In holographic setups, modular transport is a useful probe of local bulk physics. To define this transport problem, we consider a family of nearby modular Hamiltonians $H(\lambda)$ labeled by λ . Assuming we can diagonalize the Hamiltonian using a unitary vector $U(\lambda)$ as

$$D(\lambda) = U(\lambda)H(\lambda)U^\dagger(\lambda) , \quad (2.5)$$

then a change in the modular Hamiltonian can be expressed as:

$$\partial_\lambda H = [\partial_\lambda U^\dagger U, H] + U^\dagger \partial_\lambda D U . \quad (2.6)$$

The second term on the right-hand side commutes with the modular Hamiltonian and is known as a modular zero mode. We can explicitly represent the zero modes as $O = e^{i \sum_a c_a Q_a}$, where c_a are constant coefficients and $[Q_a, H] = 0$.

Transforming the modular Hamiltonian by a zero mode as

$$\tilde{H} = \tilde{U}^\dagger D \tilde{U} , \quad (2.7)$$

with $\tilde{U} = UO$, leaves (2.6) invariant. Thus the choice of zero mode frame is a gauge redundancy with an associated connection $\Gamma := P_0[\partial_\lambda U^\dagger U]$, where P_0 is a projector onto the zero mode. If we transform U by a zero mode $U \rightarrow \tilde{U} = UO$, the connection changes as

$$\Gamma \rightarrow \tilde{\Gamma} = P_0[O^\dagger \Gamma O - O^\dagger \partial_\lambda O] = P_0[-O^\dagger \mathcal{D}_\lambda O] , \quad (2.8)$$

where \mathcal{D}_λ is a covariant derivative given by

$$\mathcal{D}_\lambda O = (\partial_\lambda - \Gamma)O . \quad (2.9)$$

If we fix a gauge by setting $\tilde{\Gamma} = 0$ we obtain

$$\mathcal{D}_\lambda O = (\partial_\lambda - \Gamma)O = 0 . \quad (2.10)$$

Dropping the tildes, this leads to the following modular transport equations:

$$\begin{aligned} \partial_\lambda H - P_0[\partial_\lambda H] &= [\partial_\lambda U^\dagger U, H] \\ P_0[\partial_\lambda U^\dagger U] &= 0 . \end{aligned} \quad (2.11)$$

Considering different connections obtained by different variations and projecting out the zero mode, the modular transport equations are solved by

$$V_i = (1 - P_0)\partial_{\lambda_i}U^\dagger U . \quad (2.12)$$

We refer to V_i as the generator of modular transport. The modular curvature is then given by [15]¹

$$\mathcal{R}_{ij} := [V_i, V_j] . \quad (2.13)$$

2.2 Modular Transport in Holography

In $\text{AdS}_{d+1}/\text{CFT}_d$, modular transport is a probe of the bulk geometry from a boundary perspective. The relation between the bulk and boundary modular Hamiltonian is given by the JLMS formula [32],

$$H_{\text{bdy}} = \frac{\hat{A}}{4G_{d+1}} + H_{\text{bulk}} + \mathcal{O}(G_{d+1}) . \quad (2.14)$$

G_{d+1} is the $(d+1)$ -dimensional Newton constant and \hat{A} is the area operator of the bulk entanglement wedge associated to the subregion in the CFT. As mentioned before, when we consider vacuum states or take the limit of being close to the entangling surface, modular flow reduces to the boost Killing vector associated to the causal diamond of the subregion. We've drawn the example of $\text{AdS}_3/\text{CFT}_2$ in Figure 2.

As explained in detail in [4] (see also [14–16]), we can interpret the zero mode redundancy of the modular Hamiltonian in the bulk as a choice of a particular zero mode frame attached to an entanglement wedge. Comparing relative zero mode frames for different entanglement wedges then gives us information about the bulk curvature. Accordingly, the modular curvature can be used to directly obtain information about the bulk Riemann curvature. [4, 14] provides a formal derivation of this relationship. Our example in the context of $\text{AdS}_3/\text{CFT}_2$ is (hopefully) instructive to see explicitly how the Riemann curvature appears in the modular curvature.

Modular Transport in CFT_2

We now show how to obtain the bulk Riemann curvature using modular transport in $\text{AdS}_3/\text{CFT}_2$. We first consider the modular Hamiltonian and transport in a two-dimensional CFT, and then construct the dual quantities in pure AdS_3 , following [4].

For a two-dimensional CFT in the vacuum, the modular Hamiltonian can be constructed from the generators of the conformal algebra. We put the CFT on a cylinder

¹In [15], the general expression for the curvature also has an overall zero mode projector. We choose to omit this, since there are no non-zero mode contributions in the examples we consider in this paper.

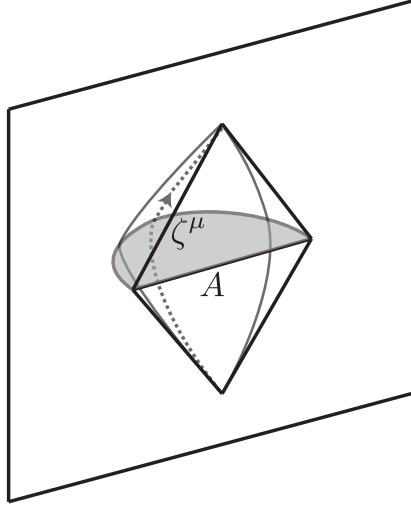


Figure 2. An interval A in a two dimensional CFT defines a causal diamond on the AdS boundary. The entanglement wedge of A defines the bulk subregion where the bulk modular Hamiltonian acts. Near the bulk entangling surface the modular Hamiltonian reduces to the (bulk) boost Killing vector ζ^μ .

and work with lightcone coordinates $x^\pm = \tau \pm \theta$, where τ is the time parameter and θ is the angle on the cylinder. The modular Hamiltonian decomposes into a left-moving and right-moving piece:

$$H = H_{(+)} + H_{(-)} . \quad (2.15)$$

Defining a conformal Killing vector (CKV) as $\zeta = \zeta^+ \partial_+ + \zeta^- \partial_-$ the modular Hamiltonian is given by

$$H_{(\pm)} = 2\pi \int dx^\pm \zeta^\pm T_{\pm\pm} , \quad (2.16)$$

where we choose a normalization of 2π in front. We use brackets in the subscript to avoid confusion with the vector components. Explicitly, we have

$$\zeta^\pm = s_1^\pm L_1^\pm + s_0^\pm L_0^\pm + s_{-1}^\pm L_{-1}^\pm , \quad (2.17)$$

where the components of the generators $L_N = L_N^+ \partial_+ + L_N^- \partial_-$ can be compactly written as

$$L_N^\pm = e^{iNx^\pm} . \quad (2.18)$$

Here, N runs over $0, \pm 1$. The generators are CKVs and therefore obey

$$\mathcal{L}_{L_N} g_{\mu\nu} - (\partial_\rho L_N^\rho) g_{\mu\nu} = 0 . \quad (2.19)$$

We now specify an interval in the CFT. We label the left endpoint by $x_i^\pm = a^\pm$ and the right endpoint by $x_f^\pm = b^\pm$. Next, we construct the modular Hamiltonian of this interval by finding the CKV that preserves the causal diamond, i.e. we want the norm of the CKV to vanish at the horizons. This vector is given by (2.17) with the coefficients

$$\begin{aligned} s_1^\pm &= \pm \frac{\cot\left[\frac{b^\pm - a^\pm}{2}\right]}{e^{ia^\pm} + e^{ib^\pm}} , \\ s_0^\pm &= \mp \cot\left[\frac{b^\pm - a^\pm}{2}\right] , \\ s_{-1}^\pm &= \pm \frac{\cot\left[\frac{b^\pm - a^\pm}{2}\right]}{e^{-ia^\pm} + e^{-ib^\pm}} . \end{aligned} \tag{2.20}$$

By taking derivatives of the modular Hamiltonian, we can construct the generators of modular transport. Instead of working with the integral representation (2.16), we opt to directly use the CKV

$$K := 2\pi\zeta . \tag{2.21}$$

The generators of modular transport are then given by

$$V_{a^\pm} = \pm \frac{1}{2\pi} \partial_{a^\pm} K , \quad V_{b^\pm} = \mp \frac{1}{2\pi} \partial_{b^\pm} K , \tag{2.22}$$

and it is straightforward to check that they solve the modular transport equations:

$$[V_{a^\pm}, K] = \partial_{a^\pm} K , \quad [V_{b^\pm}, K] = \partial_{b^\pm} K . \tag{2.23}$$

There is no zero mode that needs to be projected out, as there is no part of $\partial_\lambda K$ that commutes with K .

Just as in the integral representation of the modular Hamiltonian, we find it convenient to split $K = K_{(+)} + K_{(-)}$ where

$$K_{(+)} := 2\pi\xi^+ \partial_+ , \quad K_{(-)} := 2\pi\xi^- \partial_- . \tag{2.24}$$

In two dimensions, this notation is rather redundant since it just labels the \pm components of K . However, next when we consider AdS₃ $K_{(\pm)}$ will also involve the radial direction. The non-zero components of the modular curvature are now given by

$$\begin{aligned} \mathcal{R}_{a^+b^+} &= [V_{a^+}, V_{b^+}] = + \frac{1}{2 \sin^2\left[\frac{a^+ - b^+}{2}\right]} \frac{K_{(+)}}{2\pi} , \\ \mathcal{R}_{a^-b^-} &= [V_{a^-}, V_{b^-}] = - \frac{1}{2 \sin^2\left[\frac{a^- - b^-}{2}\right]} \frac{K_{(-)}}{2\pi} . \end{aligned} \tag{2.25}$$

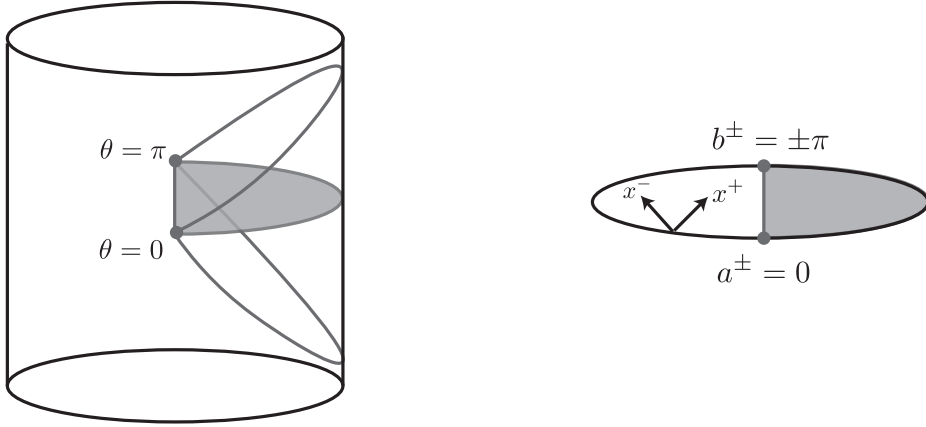


Figure 3. Global AdS_3 corresponds to a cylinder. We choose an interval in the CFT_2 that covers half of the cylinder. The Ryu-Takayanagi surface is then given by a simple diagonal geodesic.

We use $\lambda = (a^+, a^-, b^+, b^-)$ to refer to the four parameters that define our interval. We then consider an infinitesimal change $\lambda' = \lambda + d\lambda$. We can parameterize all possible changes via the following basis:

$$\begin{aligned}
\lambda_1 &= (a^+ - d\lambda, a^- - d\lambda, b^+ - d\lambda, b^- - d\lambda) , \\
\lambda_2 &= (a^+ - d\lambda, a^- + d\lambda, b^+ - d\lambda, b^- + d\lambda) , \\
\lambda_3 &= (a^+ - d\lambda, a^- - d\lambda, b^+ - d\lambda, b^- + d\lambda) , \\
\lambda_4 &= (a^+ - d\lambda, a^- - d\lambda, b^+ + d\lambda, b^- - d\lambda) .
\end{aligned} \tag{2.26}$$

The generator of modular transport for any infinitesimal deformation is a linear combination of the four generators

$$V_{\lambda_i} = \left(\frac{\partial a^+}{\partial \lambda_i} \right) V_{a^+} + \left(\frac{\partial a^-}{\partial \lambda_i} \right) V_{a^-} + \left(\frac{\partial b^+}{\partial \lambda_i} \right) V_{b^+} + \left(\frac{\partial b^-}{\partial \lambda_i} \right) V_{b^-} . \tag{2.27}$$

We now specify to an interval given by $\tau = 0$ and $\theta = [0, \pi]$ which covers half of the cylinder. This choice has the advantage that the minimal surface in the bulk corresponds to a simple diagonal geodesic, see Figure 3. In lightcone coordinates the interval is given by $[a^\pm, b^\pm] = [0, \pm\pi]$. For this choice of interval the generators for the basis (2.26) become

$$\begin{aligned}
V_{\lambda_1} &= \partial_+ + \partial_- , \\
V_{\lambda_2} &= \partial_+ - \partial_- , \\
V_{\lambda_3} &= \partial_+ + \cos(x^-)\partial_- , \\
V_{\lambda_4} &= \cos(x^+)\partial_+ - \partial_- .
\end{aligned} \tag{2.28}$$

The first two generators have an especially simple interpretation as they correspond to a translation in the τ and θ direction respectively.

Modular Transport in AdS₃

We now turn to the bulk dual of the modular transport problem described in the two-dimensional CFT. We consider the AdS₃ metric in global coordinates,

$$ds^2 = \ell^2(-\cosh^2 \rho d\tau^2 + d\rho^2 + \sinh^2 \rho d\theta^2) . \quad (2.29)$$

Lightcone coordinates in the bulk are similarly defined as $x^\pm = \tau \pm \theta$. The AdS boundary is located at $\rho \rightarrow \infty$.

The bulk modular Hamiltonian can be found by extending the CKV's of the causal diamond in the boundary to the bulk. In fact, the conformal algebra satisfied by (2.18) corresponds to the algebra satisfied by the Killing vectors (KVs) of AdS₃. The CKV in the CFT₂ is therefore the boundary value of the full bulk KV in AdS₃ that preserves the entanglement wedge.

With a slight abuse of notation, we again write $K = 2\pi\zeta$. K splits into $K_{(+)} + K_{(-)}$ which are given by

$$K_{(\pm)} = 2\pi (s_1^\pm J_1^\pm + s_0^\pm J_0^\pm + s_{-1}^\pm J_{-1}^\pm) , \quad (2.30)$$

with

$$\begin{aligned} J_1^\pm &= e^{ix^\pm} \coth(2\rho) \partial_\pm - e^{ix^\pm} \operatorname{csch}(2\rho) \partial_\mp - \frac{i}{2} e^{ix^\pm} \partial_\rho , \\ J_0^\pm &= \partial_\pm , \\ J_{-1}^\pm &= \frac{1}{2} e^{-ix^\pm} (\coth \rho + \tanh \rho) \partial_\pm - e^{-ix^\pm} \operatorname{csch}(2\rho) \partial_\mp + \frac{i}{2} e^{-ix^\pm} \partial_\rho . \end{aligned} \quad (2.31)$$

It is straightforward to check that J_N^\pm are KVs of AdS₃ and satisfy

$$\lim_{\rho \rightarrow \infty} J_N^\pm \Big|_{\partial_\rho=0} = L_N^\pm . \quad (2.32)$$

We want the KV to preserve the entanglement wedge, thus its norm needs to vanish at the horizons. This requirement is equivalent to the requirement that the CKV in the CFT₂ preserves the causal diamond, so the coefficients are again given by (2.20).

Again defining the generators of modular transport V_{a^\pm} , V_{b^\pm} as in (2.22), but with K as in (2.30), as before we find the modular transport equations (2.23). Additionally we can use the same basis (2.27) to express a general infinitesimal deformation.

Similarly, the modular curvature components are given by (2.25). Explicitly:

$$\begin{aligned}\mathcal{R}_{a^+b^+} &= [V_{a^+}, V_{b^+}] = +\frac{1}{2\sin^2\left[\frac{a^+-b^+}{2}\right]}\frac{K_{(+)}}{2\pi} , \\ \mathcal{R}_{a^-b^-} &= [V_{a^-}, V_{b^-}] = -\frac{1}{2\sin^2\left[\frac{a^-b^-}{2}\right]}\frac{K_{(-)}}{2\pi} .\end{aligned}\tag{2.33}$$

Now, $K_{(\pm)}$ refers to (2.30).

As before, choosing the diagonal geodesic $(a^\pm, b^\pm) = (0, \pm\pi)$, the entangling surface in the bulk is given by the diagonal geodesic that connects these two endpoints (as we displayed in Figure 3). For this geodesic, the generators in our basis take the form

$$\begin{aligned}V_{\lambda_1} &= \partial_+ + \partial_- , \\ V_{\lambda_2} &= \partial_+ - \partial_- , \\ V_{\lambda_3} &= (1 - \cos x^- \operatorname{csch}(2\rho))\partial_+ + \cos x^- \operatorname{coth}(2\rho)\partial_- + \frac{1}{2}\sin x^- \partial_\rho , \\ V_{\lambda_4} &= \cos x^+ \operatorname{coth}(2\rho)\partial_+ + (1 - \cos x^+ \operatorname{csch}(2\rho))\partial_- + \frac{1}{2}\sin x^+ \partial_\rho .\end{aligned}\tag{2.34}$$

Relation between Modular and Riemann Curvature

As explained in [4], the modular curvature is a probe of the Riemann curvature in the bulk. Since the modular Hamiltonian implements a boost isometry that preserves the entanglement wedge (at least near its edge), it is perhaps unsurprising that we can probe the bulk geometry by studying how this Hamiltonian changes under modular transport.

For modular Hamiltonians that reduce to a boost only near the edge of the entanglement wedge, it is convenient to set up a Riemann normal coordinate system in which the metric is flat at the boundary of the entanglement wedge. In this coordinate system, [14] derived the relation between the modular curvature and the Riemann tensor.² We demonstrate this method to obtain the Riemann curvature for three-dimensional theories using Fermi normal coordinates in Appendix A.

In this paper we will also consider modular flow for subregions that are not attached to the boundary. For a single subregion that is not attached to the boundary the modular Hamiltonian is not given by a Killing vector, but a conformal Killing vector.

We will only study situations where the modular Hamiltonian is an exact (conformal) Killing vector. In this case, the relation between the modular curvature and Riemann curvature follows more directly. It is no longer necessary to make use of a

²See (3.20) of [14]. It should be noted however that this expression contains a typo that we correct in Appendix A.

Riemann normal coordinate system. Accordingly, we define the modular Hamiltonian K of the entanglement wedge associated to a CFT_2 interval with endpoints (a^\pm, b^\pm) . We then consider an infinitesimal displacement of the entanglement wedge in the $+$ direction described by the generators V_{a^+} and V_{b^+} . For convenience, we define

$$\begin{aligned} K'_{a^+} &\equiv \frac{1}{(2\pi)^2} \partial_{a^+} K = \frac{1}{(2\pi)^2} [V_{a^+}, K] , \\ K'_{b^+} &\equiv \frac{1}{(2\pi)^2} \partial_{b^+} K = \frac{1}{(2\pi)^2} [V_{b^+}, K] . \end{aligned} \quad (2.35)$$

Absorbing the factors of 2π here results in a nice looking expression for the modular curvature below.

Using the definition of the generators (2.23), we can express

$$V_{a^+} = [K'_{a^+}, K] , \quad V_{b^+} = -[K'_{b^+}, K] . \quad (2.36)$$

By working out the commutators, the modular curvature can now be expressed as

$$\begin{aligned} (\mathcal{R}_{a^+b^+})^\mu &= [V_{a^+}, V_{b^+}]^\mu = V_{a^+}^\nu \left(2R_{\sigma\nu\rho}{}^\mu K'^{[\rho}{}_{b^+} K^{\sigma]} + \nabla_\nu K'^\rho{}_{b^+} \nabla_\rho K^\mu - \nabla_\nu K^\rho \nabla_\rho K'^\mu{}_{b^+} \right) \\ &\quad - \nabla_\nu V_{a^+}^\mu V_{b^+}^\nu . \end{aligned} \quad (2.37)$$

The appearance of the Riemann tensor is a direct consequence of the fact that K and K'_{b^+} are Killing vectors. This follows from the fact that for a general Killing vector Y we can use the identity $\nabla_\mu \nabla_\nu Y^\rho = R_{\sigma\mu\nu}{}^\rho Y^\sigma$, assuming the metric is torsion-free. This expression therefore gives a relation between the modular curvature and bulk Riemann curvature in addition to terms involving the (change of the) modular Hamiltonian.

Later on, we will study modular transport for an interval in a $1+1$ -dimensional gravitational theory. In that case, the modular Hamiltonian is given by a CKV. For that purpose, we also denote the relation when instead of Killing vectors, we only have CKVs. In that case we obtain an additional term Ω^μ (in $d+1$ -spacetime dimensions):

$$\begin{aligned} [V_{a^+}, V_{b^+}]^\mu &= V_{a^+}^\nu \left(2R_{\sigma\nu\rho}{}^\mu K'^{[\rho}{}_{b^+} K^{\sigma]} + \nabla_\nu K'^\rho{}_{b^+} \nabla_\rho K^\mu - \nabla_\nu K^\rho \nabla_\rho K'^\mu{}_{b^+} \right) \\ &\quad - \nabla_\nu V_{a^+}^\mu V_{b^+}^\nu + \frac{1}{d+1} \Omega^\mu . \end{aligned} \quad (2.38)$$

Ω^μ is defined as

$$\Omega^\mu = V_{a^+}^\nu \left[K^\rho \nabla^\mu (\nabla \cdot K'_{b^+}) g_{\nu\rho} - K^\rho \nabla_\rho (\nabla \cdot K'_{b^+}) g_\nu{}^\mu - K^\rho \nabla_\nu (\nabla \cdot K'_{b^+}) g_\rho{}^\mu - (K \leftrightarrow K'_{b^+}) \right] , \quad (2.39)$$

and vanishes when K and K'_{b+} are Killing vectors.³

This finishes our discussion of modular transport in the context of $\text{AdS}_3/\text{CFT}_2$ and the relation between the modular curvature and the Riemann curvature. Next, we specialize to a (1+1)-dimensional bulk and consider modular transport in JT gravity.

3 Modular Transport in JT Gravity

Now that we have seen how modular transport probes bulk curvature, we shift our focus to two-dimensional JT gravity. This choice has the advantage that we can incorporate the effect of quantum extremal surfaces and see—in the presence of an island—how modular transport probes geometry and entanglement of disconnected entanglement wedges. In certain simplifying limits, modular flow becomes local and the modular curvature is directly related to the Riemann curvature of the quantum extremal surface. However, in general the ‘Quantum Extremal Modular Curvature’ is a non-geometric object that captures non-local effects in the entanglement structure.

First, we start with a review of JT gravity.

3.1 JT Gravity on AdS_2

We now review a two-dimensional black hole solution in JT gravity. We start with the action of JT gravity on an AdS_2 background:

$$I = \frac{1}{16\pi G_2} \int d^2x \sqrt{-g} \left(\phi R + \frac{2}{\ell^2} (\phi - \phi_0) \right) + I_{\text{CFT}} + I_{\text{bdy}} . \quad (3.1)$$

Here I_{CFT} corresponds to a coupling to a CFT and I_{bdy} contains a boundary term. The equations of motion are

$$\begin{aligned} -\nabla_\mu \nabla_\nu \phi + g_{\mu\nu} \square \phi - \frac{(\phi - \phi_0)}{\ell^2} g_{\mu\nu} - 8\pi G_2 T_{\mu\nu} &= 0 , \\ R + 2/\ell^2 &= 0 . \end{aligned} \quad (3.2)$$

If we are interested in solutions where the dilaton exhibits a symmetry, then it is easiest to work in coordinates that preserve the same symmetry. In our case, we focus on

³To derive this relation, we used the following identity for a CKV ζ , which can be derived from the definition of curvature from parallel transport of a vector field combined with the algebraic Bianchi identity:

$$\nabla_\mu \nabla_\nu \zeta^\rho = R_{\sigma\mu\nu}{}^\rho \zeta^\sigma - \frac{1}{d} \left(\nabla^\rho (\nabla \cdot \zeta) g_{\mu\nu} - \nabla_\nu (\nabla \cdot \zeta) g_\mu{}^\rho - \nabla_\mu (\nabla \cdot \zeta) g_\nu{}^\rho \right) , \quad (2.40)$$

again assuming the metric is torsion-free.

time-independent solutions so it is appropriate to consider the AdS₂ metric in Poincaré coordinates:

$$ds^2 = \frac{\ell^2}{x^2}(-dt^2 + dx^2) . \quad (3.3)$$

We take $x \leq 0$ with $x = 0$ the AdS boundary. With this choice the non-gravitating bath region that we couple to is located at $x > 0$. This metric has a timelike Killing vector and imposing the dilaton to be invariant under this symmetry, the vacuum solution (i.e. $T_{\mu\nu} = 0$) for the dilaton is given by

$$\phi = \phi_0 - \frac{\phi_r}{x} , \quad (3.4)$$

where ϕ_0 and ϕ_r are constants.

Because left-movers and right-movers decouple in two dimensions it is convenient to introduce Kruskal coordinates

$$x^\pm = t \pm x , \quad (3.5)$$

in which the metric and dilaton solution become

$$ds^2 = -\frac{4\ell^2}{(x^+ - x^-)^2} dx^+ dx^- , \quad (3.6)$$

$$\phi = \phi_0 - \frac{2\phi_r}{x^+ - x^-} .$$

Now we allow the stress tensor to be nonzero. First, we treat this matter coupling classically. Conformal invariance then implies that the trace of the stress tensor vanishes. In this case, the equations of motion can be integrated to obtain the general solution [33, 34]

$$\phi = \phi_0 - \frac{2\phi_r}{x^+ - x^-} + 8\pi G_2 (I_+ - I_-) . \quad (3.7)$$

Here we defined the two functions

$$I_+ = \int_{x_0^+}^{x^+} ds \frac{(x^+ - s)(x^- - s)}{(x^+ - x^-)} T_{++}(s) , \quad (3.8)$$

$$I_- = \int_{x_0^-}^{x^-} ds \frac{(x^+ - s)(x^- - s)}{(x^+ - x^-)} T_{--}(s) ,$$

where the location x_0 with coordinates (x_0^+, x_0^-) is a reference point. Adjusting this point simply changes the constant ϕ_0 in (3.7).

Treating the matter sector quantum mechanically, the trace of the stress tensor no longer vanishes. Instead, for a metric written in conformal gauge,

$$ds^2 = -e^{2\omega(x^+, x^-)} dx^+ dx^- , \quad (3.9)$$

the conformal anomaly leads to a non-zero off-diagonal component on curved backgrounds:

$$\langle T_{+-} \rangle = -\frac{c}{12\pi} \partial_+ \partial_- \omega . \quad (3.10)$$

Using the conformal anomaly as input, the diagonal components can be found by integrating the continuity equation $\nabla_\mu T^{\mu\nu} = 0$ [35]

$$\langle T_{\pm\pm} \rangle = -\frac{c}{12\pi} (\partial_\pm^2 \omega - (\partial_\pm \omega)^2) + : T_{\pm\pm} : . \quad (3.11)$$

The left-hand side is the covariant stress tensor that appears on the right-hand side of the semi-classical equations of motion and the second term on the right denotes the normal-ordered stress tensor.⁴ This quantity depends on the choice of state and corresponds to left and right-moving radiation as measured by a local observer.

Using the AdS metric (3.6) we see that

$$\begin{aligned} \langle T_{\pm\pm} \rangle &=: T_{\pm\pm} : , \\ \langle T_{\pm\mp} \rangle &= \frac{c}{12\pi(x^+ - x^-)^2} . \end{aligned} \quad (3.12)$$

Taking into account the conformal anomaly the dilaton solution is just modified by a constant:

$$\phi = \phi_0 - \frac{2\phi_r}{x^+ - x^-} + 8\pi G_2 \left(I_+ - I_- + \frac{c}{24\pi} \right) . \quad (3.13)$$

Extremal Black Hole Solution

We now couple this JT gravity solution to a non-gravitational Minkowski region described by metric $ds^2 = -dx^+ dx^-$. For simplicity, we consider the CFT to be at zero temperature, which sets $: T_{\pm\pm} := 0$ and is appropriate to describe an extremal black hole [37]. We then consider an interval R whose endpoints we denote with $[a_i, b_i]$, where $i = (1, 2)$. In Kruskal coordinates a point denoted by a_i or b_i is shorthand for $x^\pm = a_i^\pm$ or $x^\pm = b_i^\pm$. When we are working at a $t = 0$ slice, we write $x = a_i$ or $x = b_i$ to denote the endpoints and drop the \pm superscript. Note that a_1 and b_1 are negative as they are located in the AdS₂ region.

We now consider an interval R at $t = 0$ given by $x \in [a_2, b_2]$ that is entangled with the bulk gravity region. To compute the fine-grained entropy of R , we use the island formula [22, 23],

$$S(R) = \min, \text{ext}_{a_1, b_1} \left(\frac{\text{Area}(\partial I)}{4G_2} + S_{\text{vN}}(R \cup I) \right) . \quad (3.14)$$

⁴Strictly speaking, normal ordering is only defined for free theories which is the case considered in this paper. More generally, one could replace $: T_{\pm\pm} :$ by a function $t_\pm(x^\pm)$ that parametrizes the flux seen by a local observer [36].

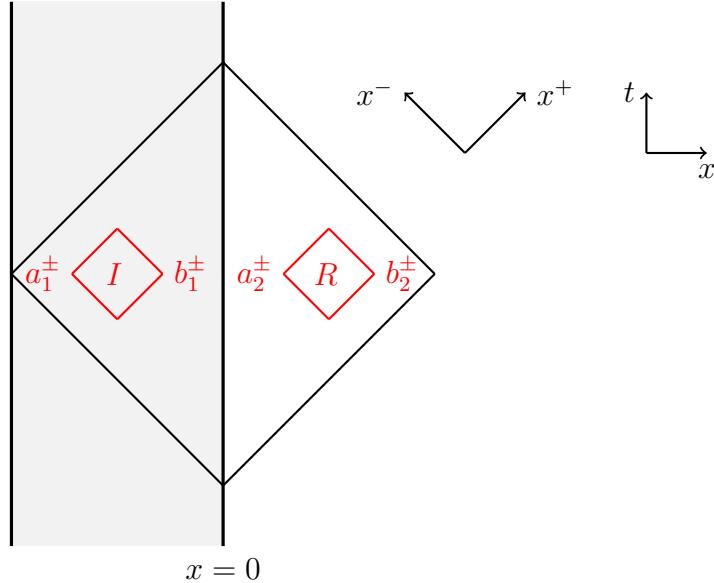


Figure 4. AdS₂ region (shaded gray) at $x \leq 0$ coupled to a flat non-gravitational bath region at $x > 0$. Two intervals are located at $t = 0$ with $x \in [a_1, b_1]$ and $x \in [a_2, b_2]$. The two diamonds indicate the domain of dependence of the two intervals.

Here we allow for an island region I located at $t = 0$ and $x \in [a_1, b_1]$ whose endpoints we extremize. This setup is depicted in Figure 4.

The von Neumann entropy of n disjoint intervals in a CFT consisting of free fermions in flat space was derived in [24]. In our case, we have two intervals; one is located in the flat bath region and the other in the AdS region. The resulting entropy can be obtained by a Weyl transformation of the flat space result. For two intervals $x = [a_1, b_1]$ and $x = [a_2, b_2]$ the flat space entropy is [24]⁵

$$S_{\text{vN}}^{\text{flat}} = \frac{c}{3} \log \left[\frac{(b_1 - a_1)(a_2 - b_1)(b_2 - a_1)(b_2 - a_2)}{(a_2 - a_1)(b_2 - b_1)\epsilon^2} \right]. \quad (3.15)$$

Transforming this result such that the interval $x = [a_1, b_1]$ is located on a background with non-trivial conformal factor we write the result in terms of the cross ratio

$$z = \frac{(b_2 - a_2)(b_1 - a_1)}{(b_2 - b_1)(a_2 - a_1)}, \quad (3.16)$$

⁵Note that (63) of [24] has a minor typo. The first sum on the second line should read: $\sum_{ij} \log |b_i - a_j|$.

in two different ways:

$$\begin{aligned}
S_{\text{vN}}(R \cup I) &= \frac{c}{3} \log \left[\frac{(b_2 - a_2)(b_1 - a_1)}{\epsilon^2 \exp(-\frac{1}{2}[\omega(a_1) + \omega(b_1)])} \right] + \frac{c}{3} \log(1 - z) , \\
&= \frac{c}{3} \log \left[\frac{(a_2 - b_1)(b_2 - a_1)}{\epsilon^2 \exp(-\frac{1}{2}[\omega(a_1) + \omega(b_1)])} \right] + \frac{c}{3} \log z .
\end{aligned} \tag{3.17}$$

The first line makes the limit $z \rightarrow 0$ easy to see, while the second does the same for the limit $z \rightarrow 1$. Here $e^{\omega(x)}$ is the conformal factor of the metric which in Poincaré coordinates in AdS₂ takes the form

$$e^{\omega(x)} = -\frac{\ell}{x} . \tag{3.18}$$

This expression for the von Neumann entropy for two intervals is specific to the free fermion theory and only takes a universal form in particular limits.

One such limit is the OPE limit $z \rightarrow 1$ where the von Neumann entropy reduces to the sum of the individual entropies of the complementary regions. Alternatively, we can consider a limit of large central charge where the entropy takes a similar form depending whether $z \lesssim \frac{1}{2}$ [38]:

$$S_{\text{vN}}(R \cup I) = \begin{cases} \frac{c}{3} \log \left[\frac{(b_2 - a_2)(b_1 - a_1)}{\epsilon^2 \exp(-\frac{1}{2}[\omega(a_1) + \omega(b_1)])} \right] & (z < \frac{1}{2}) \\ \frac{c}{3} \log \left[\frac{(a_2 - b_1)(b_2 - a_1)}{\epsilon^2 \exp(-\frac{1}{2}[\omega(a_1) + \omega(b_1)])} \right] & (z > \frac{1}{2}) . \end{cases} \tag{3.19}$$

Corrections to this large central charge result have been studied in [39]. A non-trivial island only contributes for the case $z > 1/2$ [40]. Thus, working in this regime, the fine-grained entropy is given by

$$S(R) = \min, \text{ext}_{a_1, b_1} \left(\frac{\phi(a_1) + \phi(b_1)}{4G_2} + \frac{c}{3} \log \left[\frac{(a_2 - b_1)(b_2 - a_1)}{\epsilon^2 \exp(-\frac{1}{2}[\omega(a_1) + \omega(b_1)])} \right] \right) . \tag{3.20}$$

Extremizing over (a_1, b_1) we find that there is only one (consistent) solution in which the entropy is real and the island located in the bulk region.

The location of the quantum extremal surface expressed in terms of the length scale $L := 3\phi_r/(2cG_2)$ is

$$\begin{aligned}
a_1 &= -\frac{1}{2} \left(b_2 + L + \sqrt{b_2^2 + 6b_2L + L^2} \right) , \\
b_1 &= -\frac{1}{2} \left(a_2 + L + \sqrt{a_2^2 + 6a_2L + L^2} \right) .
\end{aligned} \tag{3.21}$$

As usual in JT gravity, L measures the deviation away from pure AdS₂.

Note that when the interval in the bulk region includes the ‘natural length’ L , we can take the limit $a_2 \ll L \ll b_2$, where the island simplifies to

$$a_1 = -b_2, \quad b_1 = -L. \quad (3.22)$$

In addition to the non-trivial QES there is always a trivial (vanishing) island. In that case, the fine-grained entropy is just given by $S_{\text{vN}}(R)$. The fine-grained entropy is given by the minimum of these two contributions:

$$S(R) = \min(S_{\text{vN}}(R), S_{\text{QES}}(R)), \quad (3.23)$$

with

$$\begin{aligned} S_{\text{vN}}(R) &= \frac{c}{3} \log \left[\frac{b_2 - a_2}{\epsilon} \right], \\ S_{\text{QES}}(R) &= \frac{\phi_0 + \phi_r/L}{2G_2} + \frac{\phi_r}{4G_2 L} \log \left[\frac{4b_2 \ell^2 L}{\epsilon^4} \right]. \end{aligned} \quad (3.24)$$

One peculiar feature of this two-dimensional model of an extremal black hole is that its island lies *outside* the black hole horizon [37]. Consequently, the modular curvature we will study later also only probes the region outside the horizon. However, for a generic model of an evaporating black hole in JT gravity, such as originally studied in [22, 23], the location of the island is behind an horizon. Applying our method to these (more complicated) models should yield (geometrical) information behind horizons.

Now that we have reviewed JT gravity including its islands, we will next construct the associated modular Hamiltonian. We will perform modular transport in two cases; both for a single interval and for the two-interval island case.

3.2 Modular Transport for a Single Interval

Similar to holography in higher dimensions, in JT gravity we can consider the bulk AdS₂ dual of the boundary modular Hamiltonian defined in the CFT₁. The relation between the bulk and boundary modular Hamiltonians is given by a two-dimensional version of the JLMS formula [32]:

$$H_{\text{bdy}} = \frac{\hat{A}}{4G_2} + H_{\text{bulk}} + \mathcal{O}(G_2). \quad (3.25)$$

Here \hat{A} is the area operator and H_{bulk} is the bulk modular Hamiltonian which acts on the matter fields.

To get some intuition for this expression, we consider the two-dimensional analogue of an RT surface, which is a single point that we denote by $x^\pm = a^\pm$. From this point,

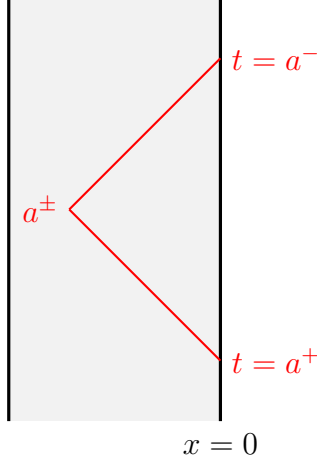


Figure 5. Two-dimensional analogue of an RT surface, which is a single point. From this point we shoot two lighttrays to define a causal diamond. This defines a time interval on the AdS boundary.

we shoot lighttrays to the boundary to form a causal diamond, as in Figure 5. Taking the state of the two-dimensional bulk matter to be the vacuum, i.e. $T_{\pm\pm} := 0$, the bulk modular Hamiltonian acts as the boost Killing vector that leaves the diamond invariant. We note that in this section we do not impose that the interval defining the diamond lies on a $t = 0$ slice. The vector field preserving the diamond is given by

$$\zeta^\mu \partial_\mu = \frac{(a^+ - x^+)(a^- - x^+)}{a^+ - a^-} \partial_+ + \frac{(a^+ - x^-)(a^- - x^-)}{a^+ - a^-} \partial_- . \quad (3.26)$$

Thus, using (2.4), the bulk modular Hamiltonian takes the form

$$H_{\text{bulk}} = 2\pi \left(\int_{a^+}^{\frac{1}{2}(a^+ + a^-)} ds \frac{(a^+ - s)(a^- - s)}{a^+ - a^-} T_{++}(s) - \int_{a^-}^{\frac{1}{2}(a^+ + a^-)} ds \frac{(a^+ - s)(a^- - s)}{a^+ - a^-} T_{--}(s) \right) , \quad (3.27)$$

which we recognize as the part of the dilaton solution coupled to the CFT_2 evaluated at $(x^+, x^-) = (a^+, a^-)$. We can now make the following identification [41, 42]:

$$H_{\text{bdy}} = \frac{\hat{\phi}}{4G_2} , \quad (3.28)$$

which relates

$$\begin{aligned} \langle \hat{A} \rangle &= \phi_0 - \frac{2\phi_r}{a^+ - a^-} , \\ \langle H_{\text{bulk}} \rangle &= 2\pi (I_+ - I_-) . \end{aligned} \quad (3.29)$$

Here we dropped the constant piece given by the central charge, which will drop out of the generators of modular transport. The area term is the Noether charge associated with the Killing vector that preserves the diamond, evaluated at the bulk point (see e.g. Appendix C of [43]). Thus, just as in higher-dimensional cases, boundary modular flow equals bulk modular flow.

We are now interested in studying the behavior of the modular Hamiltonian in the presence of an island. As before, we couple the AdS₂ bulk to a non-gravitating bath region, see Figure 4. When we consider an interval in the bath in the presence of an island, the boundary modular Hamiltonian is given by an expression similar to the island formula for the fine-grained entropy [25]:

$$H_{\text{bdy}} = \frac{\hat{A}(\partial I)}{4G_2} + H_{\text{bulk}}(A \cup I) . \quad (3.30)$$

A remarkable property this island generalization of the JLMS formula is that the left-hand side is proposed to be the exact fine-grained modular Hamiltonian associated to the quantum state of the boundary theory, but the right-hand side is an expression evaluated in the semi-classical gravity theory. Apparently, semi-classical gravity has access to some fine-grained information of the full theory. Accordingly, we can evaluate the modular Hamiltonian, just by knowing its form in the semi-classical theory.

Evaluated on a trivial island ($I = \emptyset$), (3.30) reduces to the matter modular Hamiltonian in the non-gravitational bath. In the presence of a non-trivial island, we instead have to understand the modular Hamiltonian of two disjoint intervals. In general, this two-interval modular Hamiltonian is a complicated non-local expression whose closed form is only known in special cases. In Sec. 3.3 we therefore consider a matter sector which consists of free massless fermions, for which the modular Hamiltonian has been derived in [24]. Before doing so, we first consider a single interval in the bulk and explicitly show how (bulk) modular transport probes the Riemann curvature.

Modular Curvature of a Bulk Interval

We now fix an interval in the bulk that defines a causal diamond. We then consider the modular Hamiltonian associated to this diamond and show how its modular curvature is related to the Riemann curvature. We stress that this is a toy example, because we define the bulk diamond just by fixing its endpoints in a gravitational theory. This is not diffeomorphism invariant and the resulting expressions might therefore be gauge dependent. Still, this will be an instructive example because the resulting expressions will naturally translate to the situation where we consider an island which we do define in a diff-invariant manner by specifying an interval in the bath region.

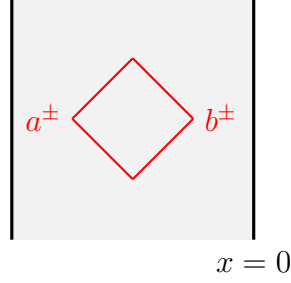


Figure 6. Causal diamond in the bulk associated to the interval $x^\pm = [a^\pm, b^\pm]$.

Keeping in mind this subtlety, we now show how the bulk Riemann curvature can be obtained from modular transport when we consider a causal diamond in the bulk. The endpoints of the interval specifying the causal diamond are given by $x^\pm = [a^\pm, b^\pm]$, see Figure 6. In vacuum, the matter modular Hamiltonian is given by the expression (2.4) where ζ^μ is the conformal Killing vector that preserves the diamond, i.e.

$$\zeta^\mu \partial_\mu = \frac{(a^+ - x^+)(b^+ - x^+)}{a^+ - b^+} \partial_+ - \frac{(a^- - x^-)(b^- - x^-)}{a^- - b^-} \partial_- . \quad (3.31)$$

We note that the KV (3.26) that preserves the half diamond attached to the boundary is a special case of this general CKV evaluated at $b^\pm = a^\mp$. (3.31) is the conformal Killing vector for any two-dimensional metric written in conformal gauge:

$$ds^2 = -e^{2\omega(x^+, x^-)} dx^+ dx^- . \quad (3.32)$$

We will now show how the bulk modular Hamiltonian can be used to probe the curvature. As before, we choose to represent the modular Hamiltonian directly by the conformal Killing vector, i.e.

$$K = 2\pi \zeta^\mu \partial_\mu . \quad (3.33)$$

We split this vector into a left-moving and right-moving piece:

$$K = K_{(+)} + K_{(-)} . \quad (3.34)$$

Focusing on the + sector the generators of modular transport are now given by

$$\begin{aligned} V_{a^+} &= +\frac{1}{2\pi} \partial_{a^+} K , \\ V_{b^+} &= -\frac{1}{2\pi} \partial_{b^+} K , \end{aligned} \quad (3.35)$$

with similar expressions for V_{a^-}, V_{b^-} . They obey the expected commutation relations of modular scrambling modes [14],

$$[V_{a^+}, K] = +2\pi V_{a^+} , \quad [V_{b^+}, K] = -2\pi V_{b^+} . \quad (3.36)$$

The modular curvature is now computed to be

$$\mathcal{R}_{a^+b^+} := [V_{a^+}, V_{b^+}] = \frac{2}{(a^+ - b^+)^2} \left(\frac{K_{(+)}}{2\pi} \right). \quad (3.37)$$

To relate the modular curvature to the Riemann curvature, we can use (2.38). Because (3.31) is the CKV of a causal diamond in any two-dimensional metric, this gives a result that is valid in general. As before, we express the change in the modular Hamiltonian in terms of K'_{a^+} , K'_{b^+} defined as:

$$K'_{a^+} = \frac{1}{(2\pi)^2} [V_{a^+}, K], \quad K'_{b^+} = \frac{1}{(2\pi)^2} [V_{b^+}, K]. \quad (3.38)$$

Evaluating the right-hand side of (2.38) we find that this expression simplifies and reduces to

$$\mathcal{R}_{a^+b^+}^+ = V_{a^+}^+ R_{-++}^+ K_{b^+}'^+ K^- - \nabla_+ V_{a^+}^+ V_{b^+}^+ + \frac{1}{2} \Omega^+. \quad (3.39)$$

This equation relates the modular curvature of a single interval in any two-dimensional spacetime to its Riemann curvature.

We will now show how the presence of an island modifies the modular curvature.

3.3 Modular Transport in the Presence of an Island

We will now study modular transport in the presence of a non-trivial quantum extremal surface. Before doing so, let us first reiterate the general idea. We consider a gravitating two-dimensional AdS space glued to a non-gravitating flat ‘bath’ region. Using modular transport in the bath region we want to understand if we can extract the bulk Riemann curvature associated to an island region, using the JLMS relation including the possibility of an island (3.30).

Similar to the island formula that computes the fine-grained entropy of Hawking radiation, (3.30) states that the *exact* modular Hamiltonian of a subregion of the bath (which is unknown in general) equals a simpler semi-classical expression involving the semi-classical bulk modular Hamiltonian of two disjoint intervals. For generic matter, the modular Hamiltonian of disjoint intervals is unknown. However, for free fermion theories, [24] derived an explicit formula. Consequently, we will now restrict to this case.

Modular Hamiltonian of Disjoint Intervals

The modular Hamiltonian of free fermions on n disjoint intervals in $1 + 1$ -dimensional flat space was derived in [24]. This model has been studied in the context of quantum extremal surfaces in [25] and modular transport in [26]. The latter reference makes use

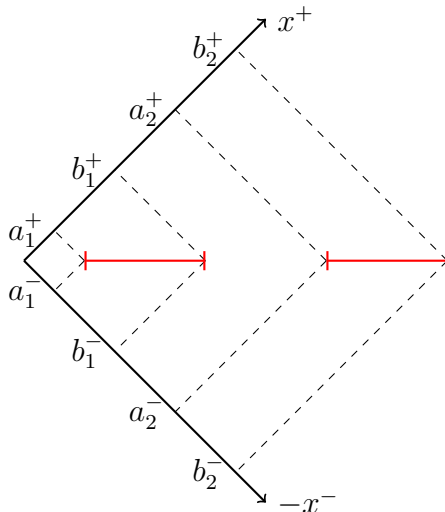


Figure 7. Two disjoint intervals whose endpoints are labeled by lightcone coordinates.

of an isomorphism—referred to as a multi-local symmetry—to transform the complicated non-local expression of the modular Hamiltonian of two disjoint intervals into a tractable local expression for two fermions on a half line where modular flow acts as a boost.

We focus on two intervals and label the endpoints as indicated in Figure 7. We first consider the non-gravitational case where these two intervals are located on flat space. As we will argue, the generalization to AdS_2 is straightforward; for our purpose of studying modular flow, it is actually essentially unmodified from the flat space case. The modular Hamiltonian splits into two pieces: $H = H_{(+)} + H_{(-)}$. In two dimensions the left and right-moving sector completely decouple so it suffices to just consider one sector. We focus on the x^+ sector, and instead of keeping track of the superscript, we just write x . We then have [24, 26]

$$H_{(+)} = 2\pi \int dx (h_T(x)T(x) + h_C(x)\psi^\dagger(x)\psi(\tilde{x})) . \quad (3.40)$$

The coefficients of the operators and the map $\tilde{x}(x)$ are

$$\begin{aligned} h_T(x) &= (\partial_x y(x))^{-1} , \\ h_C(x) &= \frac{\partial_x \tilde{x}}{x - \tilde{x}} h_T(x) , \\ y(x) &= \log \left[-\frac{(x - a_1)(x - a_2)}{(x - b_1)(x - b_2)} \right] , \\ \tilde{x}(x) &= \frac{a_1 a_2 (x - b_1 - b_2) - b_1 b_2 (x - a_1 - a_2)}{(a_1 + a_2 - b_1 - b_2)x - a_1 a_2 + b_1 b_2} , \end{aligned} \quad (3.41)$$

and the fermion stress tensor is given by

$$T(x) = \frac{1}{2} (\partial_x \psi^\dagger \psi - \psi^\dagger \partial_x \psi) . \quad (3.42)$$

Since we are focusing on the + sector, the coefficients a_i, b_i refer to the + components. The map $\tilde{x}(x)$ is quasi-local in the sense that it exchanges points in the two intervals. The second term in the modular Hamiltonian therefore couples fermions non-locally, but point wise. This fact was used in [25] to understand how an operator in an island region can be mapped to a bath region under modular flow.⁶

To highlight the difference between the local modular Hamiltonian for a single interval and its non-locality for disjoint intervals, we display the evolution of the local fermion operators under modular flow. For this purpose it is useful to consider the function $y(x)$ defined in (3.41). This function runs from $[-\infty, +\infty]$ in each interval $[a_1, b_1]$ and $[a_2, b_2]$. A value of $y(x)$ corresponds to one point in each interval, which we denote by $x_i(y)$. We can then define a fermion operator in each interval as

$$\tilde{\psi}_i(y) := \sqrt{\frac{dx_i}{dy}} \psi(x_i(y)) . \quad (3.43)$$

Under modular flow, the positions of the operators evolve with the modular time parameter s as $y(s) = y(0) + 2\pi s$ and the operators transform as [24]

$$\psi_i(y(s)) = R_i^j \psi_j(y(0)) . \quad (3.44)$$

Here R is a rotation matrix

$$R_i^j = \begin{pmatrix} \cos \theta(s) & -\sin \theta(s) \\ \sin \theta(s) & \cos \theta(s) \end{pmatrix} , \quad (3.45)$$

with angle

$$\theta(s) = \left[\arctan \left(\frac{(b_1 + b_2 - a_1 - a_2)x_1(s) + (a_1 a_2 - b_1 b_2)}{\sqrt{(b_1 - a_1)(a_2 - b_1)(b_2 - a_1)(b_2 - a_2)}} \right) - (s = 0) \right] . \quad (3.46)$$

Specifying an initial condition $y(0)$, this relation can be inverted to obtain the position of the operators under modular flow.

Fixing the length of both diamonds to be equal, we demonstrate the behavior of modular flow in three illustrative examples in Figures 8, 9 and 10. We notice that for

⁶The reference [25] uses different conventions to label the intervals. The relation between our and their conventions is given by $(a_{1,2}^+, b_{1,2}^+)_{\text{us}} \rightarrow (a_{1,2}^+, b_{1,2}^+)_{\text{them}}$ and $(a_{1,2}^-, b_{1,2}^-)_{\text{us}} \rightarrow (b_{2,1}^-, a_{2,1}^-)_{\text{them}}$. Thus, for our focus on the + sector, the two conventions coincide.

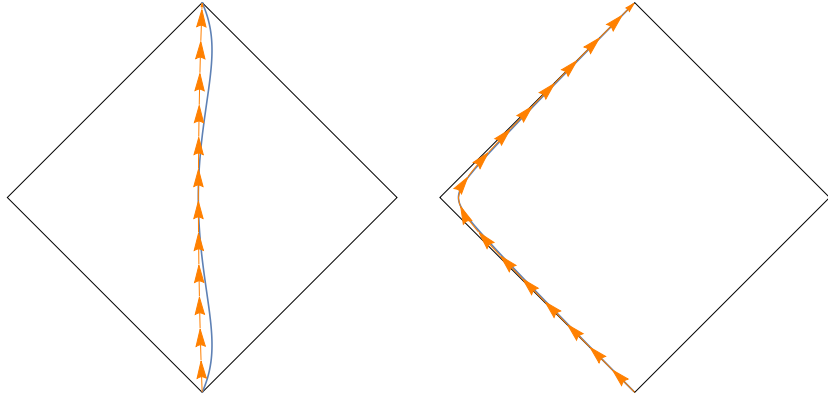


Figure 8. Behavior of the position of the operators $\tilde{\psi}_i(y)$ under modular flow. The blue line corresponds to the modular flow trajectory and the orange trajectory corresponds to the CKV of each diamond. We see that, in general, modular flow in the bulk of the diamond does not coincide with the flow of the CKV of the diamond. Close to the edge of the diamond, however, they do coincide. We took $[a_1, b_1] = [-0.01, 0.99]$, $[a_2, b_2] = [1.1, 2.1]$ and $y(0) = -1$.

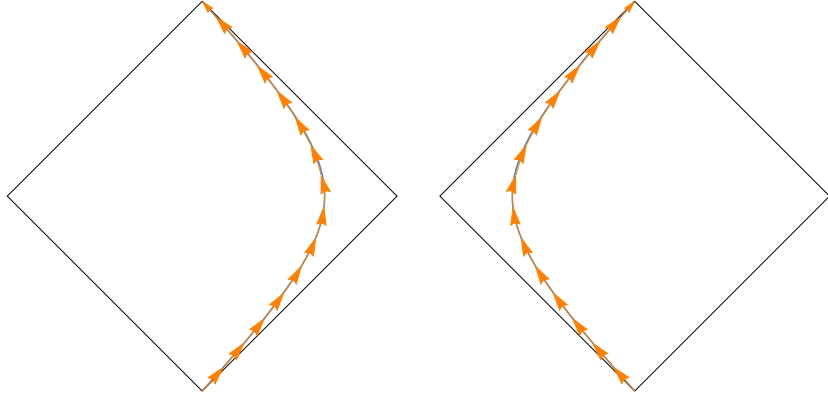


Figure 9. Behavior of the position of the operators $\tilde{\psi}_i(y)$ under modular flow. The blue line corresponds to the modular flow trajectory and the orange trajectory corresponds to the CKV of each diamond. If we consider operators close to the edge of the diamond, the modular flow trajectory coincides with the CKV of the diamond. We took $[a_1, b_1] = [-0.01, 0.99]$, $[a_2, b_2] = [1.1, 2.1]$ and $y(0) = 0$.

diamonds that are far away from other, modular flow follows the trajectory of the CKV of the diamond. Indeed, this is also easy to see analytically. In the limit where the cross-ratio $z \rightarrow 0$, the non-local piece of the modular Hamiltonian vanishes. One way of taking this limit is by shrinking one of the intervals to zero size, let's say $a_2 \rightarrow b_2$.



Figure 10. Behavior of the position of the operators $\tilde{\psi}_i(y)$ under modular flow. We note that modular flow couples points at different values $y(x)$ in each interval. The blue line corresponds to the modular flow trajectory and the orange trajectory corresponds to the CKV of each diamond. When the diamonds are far away from each other the modular flow trajectory coincides with the CKV of the diamond. We took $[a_1, b_1] = [-0.01, 0.99]$, $[a_2, b_2] = [2, 3]$ and $y(0) = -1$.

The modular Hamiltonian then becomes the CKV of the remaining interval:

$$\begin{aligned} \lim_{a_2 \rightarrow b_2} h_T(x) &= \frac{(a_1 - x)(b_1 - x)}{a_1 - b_1}, \\ \lim_{a_2 \rightarrow b_2} h_C(x) &= 0. \end{aligned} \tag{3.47}$$

In addition, the figures also make it clear that modular flow follows the trajectory of a CKV when we consider an operator that is close to the edge of the diamond. This behavior seems similar to the fact that the modular Hamiltonian of excited states reduces to the boost Killing vector close to the boundary, although here there still is a non-local piece. Thus, the operators $\tilde{\psi}_1(y)$ and $\tilde{\psi}_2(y)$ still mix but their trajectories are described by the CKV of their respective diamonds.

In principal, one can obtain the generators of modular transport by varying (3.40). However, away from a simplifying limit where the non-local piece vanishes, this procedure quickly becomes unwieldy when studying modular transport. For this reason, in cases where the non-local contribution cannot be dropped, it is more convenient to make use of the multi-local symmetry utilized in [26] to obtain a more tractable expression for the modular Hamiltonian that is local. The map to a local modular Hamiltonian involves an isomorphism β that maps two species of fermion $\Psi_{i=1,2}$ on a half-line $I = [0, \infty]$ to a single fermion ψ on two disjoint intervals $I_1 \cup I_2 = [a_1, b_1] \cup [a_2, b_2]$. This

map involves a coordinate transformation to ‘ X -space’:⁷

$$X(x) = -\frac{(x-a_1)(x-a_2)}{(x-b_1)(x-b_2)}. \quad (3.48)$$

It has two inverses $x_{1,2}(X)$, which send the half-line $[0, \infty]$ to either the interval $[a_1, b_1]$ or $[a_2, b_2]$. For more details regarding this multi-local symmetry we refer the reader to [26, 44]. Here we just note that the map β acts on fermions in X -space as:

$$\begin{aligned} \beta[\Psi_i(X)] &= \sum_{j=1,2} U_{ij} \sqrt{\partial_X x_j(X)} \psi(x_j(X)) , \\ \beta[\Psi_i^\dagger(X)] &= \sum_{j=1,2} U_{ij} \sqrt{\partial_X x_j(X)} \psi^\dagger(x_j(X)) , \end{aligned} \quad (3.49)$$

where $U = e^{c\Theta(X)}$ is an orthogonal matrix. The parameter $\Theta(X)$ is defined as

$$\Theta(X) = \int^X dY \frac{\sqrt{\partial_Y x_1(Y) \partial_Y x_2(Y)}}{x_1(Y) - x_2(Y)} , \quad (3.50)$$

and implements a gauge transformation that introduces a monodromy around the branch points of the map $X(x)$.

To explicitly evaluate the action of the map, it will be useful to expand $U_{ij} = \delta_{ij} + \epsilon_{ij}\Theta(x) + \dots$, where ϵ_{ij} is the Levi-Civita symbol. The inverse map β^{-1} acts on $H_{(+)}$ as

$$\beta^{-1} \circ H_{(+)} = 2\pi \int dX X (T_{11}(X) + T_{22}(X)) . \quad (3.51)$$

We see that in X -space the modular Hamiltonian simply acts as a boost on the two fermions defined in Rindler space. The stress tensors of the two fermions are given by

$$T_{ij}(X) = \frac{1}{2} \left(\partial_X \Psi_i^\dagger(X) \Psi_j(X) - \Psi_i^\dagger(X) \partial_X \Psi_j(X) \right) . \quad (3.52)$$

Varying (3.51) gives a more tractable way of obtaining the generators of modular transport.

Modular Transport with Islands

The expressions for the modular Hamiltonian and modular transport that we just presented are valid on flat space. However, our setup of interest consists of one (bath) interval located on flat space and one on AdS_2 . Nonetheless, because we consider the fermion in the vacuum state, i.e. $:T_{\pm\pm}: = 0$, we can see from (3.10) and (3.11) that

⁷We refer to the representation (3.40) as x -space, which is the same as the z -space in [26].

the only difference between the stress tensor on flat space and AdS₂ is the conformal anomaly. This contribution can be safely dropped to study the dynamics of the modular Hamiltonian, such that we can readily apply the expression for the modular Hamiltonian on flat space to our situation of interest.

Now we will take some interesting limits. We first evaluate the modular Hamiltonian on the location of the island, given by (3.21). Working in the limit $a_2/L \ll 1$ and $b_2/L \gg 1$, keeping L fixed, the location of the island is simply given by $(a_1, b_1) = (-b_2, -L)$. Since we are working with a CFT in the vacuum, we can equivalently describe this situation in terms of the complement of the two intervals which, in this limit, is just a single interval. We then expect the modular Hamiltonian to reduce to the single interval result, i.e. it should implement a boost with respect to the CKV of the causal diamond defined by the interval $x = [-L, 0]$. Indeed, taking this limit we obtain

$$h_T(x)_{\text{QES}} = \frac{x(L+x)}{L}, \quad (3.53)$$

which corresponds to minus the $+$ component of the CKV of the diamond associated to the interval $x = [-L, 0]$. As anticipated, this interval is the complement of the $[a_1, b_1] \cup [a_2, b_2]$ after imposing the QES condition and taking the limit $a_2/L \ll 1$ and $b_2/L \gg 1$.

Because in this limit the modular Hamiltonian reduces to the CKV of the diamond $x = [-L, 0]$, we expect to be able to still extract the Riemann curvature using modular transport. This expectation is essentially true, up to a subtlety involving the non-local contribution. Taking the same limit in the non-local coefficient, we obtain

$$h_C(x)_{\text{QES}} = \frac{2x(L+x)}{L(L+2x)}. \quad (3.54)$$

Perhaps surprisingly, this term is non-zero. One should be careful however in interpreting this result, as the map $\tilde{x}(x)$ becomes ill-defined in this limit as one interval has reduced to a point. Thus, the non-local coupling $\psi^\dagger(x)\psi(\tilde{x})$ needs to be reinterpreted. Said differently, considering the modular Hamiltonian of a single interval and taking the single-interval limit of the two-interval modular Hamiltonian do not commute. Later, we will show that in X -space the single interval limit is regular and non-local contributions to modular transport vanish. For now, we will therefore simply ignore the non-local contribution.

After varying the modular Hamiltonian (3.40), [26] obtained the generators of modular transport. As mentioned, for now we only keep the local terms.⁸ The complete generators (including non-local terms) are displayed in Appendix B.

⁸This amounts to only keeping the first term proportional to $T(x)$ in (B.1).

As in the AdS₃/CFT₂ case, we define a left-moving and right-moving piece of the (local) modular Hamiltonian as $K = K_{(+)} + K_{(-)}$ with

$$K_{(\pm)} = \pm 2\pi h_T(x^\pm) \partial_\pm . \quad (3.55)$$

In the single interval limit we are considering the non-zero generators are (where we dropped the + superscript on b_1, a_2)

$$\begin{aligned} V_{b_1} &= -\frac{1}{2\pi} \partial_{b_1} K_{(+)} , \\ V_{a_2} &= +\frac{1}{2\pi} \partial_{a_2} K_{(+)} . \end{aligned} \quad (3.56)$$

We now obtain the expected commutation relations

$$[V_{b_1}, K] = \partial_{b_1} K , \quad [V_{a_2}, K] = \partial_{a_2} K . \quad (3.57)$$

The only non-zero component of the modular curvature is given by

$$\mathcal{R}_{a_2 b_1} = \frac{2}{L^2} h_T(x) . \quad (3.58)$$

We recognize this expression as $2/(2\pi L^2)$ times the modular Hamiltonian. The coefficient is indeed $2/(b_1 - a_2)^2$ evaluated on the island, as expected. Using the relation (3.39) we can now relate this modular curvature to the Riemann curvature.

Due to the generalization of the JLMS relation to include a possible island (see (3.30)), we see that it is possible to reconstruct the Riemann curvature far away from the bath region by acting with the exact generator of modular transport. Concretely, let us define the generator $V_{a_2}^Q$ in the exact theory. This generator is a complicated operator that (non-perturbatively) has information about the bulk. To distinguish the modular curvature computed using the generators $V_{a_2}^Q$ and $V_{b_2}^Q$ from the modular curvature in the semi-classical theory we refer to any commutator of an exact generator with another generator as the Quantum Extremal Modular Curvature (QEMC). Knowledge of this operator allows an observer in the boundary theory to extract geometrical information of islands in the bulk using the QEMC. Concretely, assuming the presence of an island in the semi-classical theory, $V_{a_2}^Q$ generates modular transport on the two disjoint intervals:

$$V_{a_2}^Q = V_{a_2} + \left(\frac{\partial b_1}{\partial a_2} \right) V_{b_1} . \quad (3.59)$$

Accordingly, in the semi-classical theory, changing the endpoint of the bath interval also changes the location of the island via the QES condition. In the limit where the

semi-classical generators are local, an observer in the exact theory can now obtain the Riemann curvature by computing

$$[V_{a_2}, V_{a_2}^Q] = \left(\frac{\partial b_1}{\partial a_2} \right) [V_{a_2}, V_{b_1}] = (-2) \mathcal{R}_{a_2 b_1} . \quad (3.60)$$

Here $\mathcal{R}_{a_2 b_1}$ is the modular curvature in the semi-classical theory. The factor of (-2) comes from the Jacobian.

This commutator might look a bit funny, since it involves the same endpoint a_2 . However, other commutators involving one exact generator just reduce to their semi-classical values, i.e. $[V_{a_2}, V_{b_2}^Q] = [V_{a_2}, V_{b_2}]$ and $[V_{b_2}, V_{a_2}^Q] = [V_{b_2}, V_{a_2}]$, and don't probe the bulk region. Using the relation between the (local) modular curvature and Riemann curvature, i.e. (3.39), we now see how the QEMC can be used to extract the Riemann curvature from modular flow. So far, we've worked in the limit where the generators of modular transport become local and saw how we could extract the Riemann curvature. Next, we go beyond this limit and compute the leading corrections to the geometric modular flow.

Beyond Geometric Flow

To compute the leading corrections to the geometric limit of the QEMC considered so far, we will make use of the multi-local symmetry we described before. This symmetry allows for tractable expressions of the generators of modular transport. To compute the leading correction to the geometric expression for the modular curvature, we still consider the same commutator in the presence of an island, i.e.

$$[V_{a_2}, V_{a_2}^Q] = \left(\frac{\partial b_1}{\partial a_2} \right) [V_{a_2}, V_{b_1}] = \left(\frac{\partial b_1}{\partial a_2} \right) \mathcal{R}_{a_2 b_1} , \quad (3.61)$$

but now we consider the generators in X -space. The explicit expressions are given in Appendix B. We then expand to leading order in an expansion of $a_2/L \ll 1$ and $b_2/L \gg 1$. Writing the commutator of interest in terms of the different zero modes that contribute we have:

$$[V_{a_2}, V_{a_2}^Q] = -\frac{4}{L^2} \left[Q_{22}^{(1)} + \sqrt{\frac{L}{8b_2}} \left(Q_{21}^{(0)} - Q_{12}^{(0)} + 2 \left(Q_{12}^{(1)} + Q_{21}^{(1)} - Q_{21}^{(2)} \right) \right) \right] . \quad (3.62)$$

The different zero modes are given by

$$\begin{aligned} Q_{ij}^{(0)} &= \int dX \Psi_i(X) \Psi_j(X) , \\ Q_{ij}^{(1)} &= \int dX X T_{ij}(X) , \\ Q_{ij}^{(2)} &= \int dX X^2 \left(\partial_X \Psi_i^\dagger(X) \partial_X \Psi_j(X) - (i \leftrightarrow j) \right) . \end{aligned} \quad (3.63)$$

The first term in the expansion is proportional to just $Q_{22}^{(1)}$ and does not involve the fermion Ψ_1 . As promised, we now see that—when transformed back to a *single* interval in x -space—the first term also has a local interpretation as a boost implemented by a CKV. Explicitly, when acting with the map β on the zero mode $Q_{22}^{(1)}$ to transform back to x -space, the term involving a derivative of the gauge parameter $\Theta(X)$ becomes proportional to the term $\psi^\dagger(x)\psi(\tilde{x})$. We find that $\Theta'(X)$ vanishes in the limit $a_2/L \ll 1$ and $b_2/L \gg 1$.⁹ Thus, the first term in (3.62) agrees with (3.60). The other terms involving couplings between the different fermions are non-local in x -space, don't have a geometric interpretation, and vanish in the limit $b_2/L \rightarrow \infty$.

One last interesting question that we want to discuss is what information we obtain from the QEMC involving two exact generators, i.e. $\mathcal{R}_{a_2 b_2}^Q = [V_{a_2}^Q, V_{b_2}^Q]$. With the expressions for the generators of modular transport in the semi-classical theory, this is easily obtained. First, let us consider the situation without an island. In this case, there is just a single interval in the bath and modular flow is completely local. In this case, we obtain the single-interval result given by

$$\text{No Island:} \quad \mathcal{R}_{a_2 b_2}^Q = \mathcal{R}_{a_2 b_2} = \frac{2}{(a_2 - b_2)^2} Q_{11}^{(1)}. \quad (3.64)$$

This expression is local, since it only involves the fermion Ψ_1 . We recognize the prefactor as the coefficient of the modular curvature of a single interval in the bulk.

Now consider the situation with an island present. In that case, we can make use of the expression of the generators in X -space to find¹⁰

$$\mathcal{R}_{a_2 b_2}^Q = [V_{a_2}, V_{b_2}] + \left(\frac{\partial b_1}{\partial a_2} \right) \left(\frac{\partial a_1}{\partial b_2} \right) [V_{b_1}, V_{a_1}]. \quad (3.65)$$

The general result looks rather complicated. Expanding for $a_2/L \ll 1$ and $b_2/L \gg 1$ we find that the leading order term in the expansion vanishes. Because we saw that in this limit modular flow becomes local in the diamond $x = [-L, 0]$, the vanishing of the leading order term implies that this component of the QEMC contains purely non-local information. The first non-zero order in the expansion is $\mathcal{O}(L/b_2)^{3/2}$. We find

$$\text{With Island:} \quad \mathcal{R}_{a_2 b_2}^Q = -\frac{1}{\sqrt{8b_2^3 L}} \left(Q_{12}^{(0)} - Q_{21}^{(0)} - 6 \left(Q_{12}^{(1)} + Q_{21}^{(1)} \right) + 2Q_{21}^{(2)} \right). \quad (3.66)$$

Indeed, this term is purely non-local and represents non-geometric information. We therefore see that $\mathcal{R}_{a_2 b_2}^Q$ only has a local interpretation in the absence of an island and becomes non-local whenever a non-trivial QES contributes.

⁹Using the language of [44], in X -space the non-local coupling is manifest by a coupling of the form $\epsilon_{ij} A^+ \Psi_i^\dagger \Psi_j$, where A^+ is a gauge field. In the limit we consider, the gauge field vanishes.

¹⁰The commutators $[V_{a_i}, V_{a_j}] = [V_{b_i}, V_{b_j}] = 0$.

4 Discussion

In this paper, we studied modular transport in JT gravity coupled to a non-gravitational bath in the presence of an island. Due to the non-trivial island, performing modular flow on this system involves two disjoint intervals: one in the gravitating bulk and one in the non-gravitating bath. In order to use analytical expressions, we coupled the JT theory to a two-dimensional free fermion theory for which the exact modular Hamiltonian was derived in [24]. Using a two-dimensional version of the JLMS formula—including the possibility of a non-trivial quantum extremal surface—we were able to define the ‘fine-grained’ generators of modular transport associated to an interval in the non-gravitational bath region. In the semi-classical theory these generators act on both the bulk and bath interval. We computed the modular curvature from these generators, which we refer to as the Quantum Extremal Modular Curvature, or QEMC.

The QEMC is non-local in general, but in a certain simplifying limit reduces to the known (local) result for a single interval in the bulk. In this limit, the QEMC probes the bulk Riemann curvature of this interval in a similar fashion as previous studies [4, 14] of the modular curvature in holography without islands. The upshot of our approach, however, is that it probes the Riemann curvature in a region that can be far away from the boundary. Thus, an observer in the bath can use this approach to obtain geometrical information about far-separated regions, possibly behind horizons.

While we performed our analysis in the context of a low-dimensional model with many simplifying features in order to have analytical control, we expect this upshot to remain true more generally: it simply relies on the fact that the location of the island is tied to the location of the interval in the bath region, by virtue of the QES condition. Thus, performing transport with respect to the bath interval necessarily results in transport of the island, which can be used to probe the local curvature in that region. In particular, there is no obvious obstruction to applying our method to a more complicated model of an evaporating black holes, such as the one studied in [22, 23], for which the island lies behind a horizon. Coupling the JT solution to the free fermion model, the modular Hamiltonian is given by the same expression we studied in this paper.

Although possible in principle, the modular transport protocol we described might be difficult to perform in practice. An observer would need to be able to compute the fine-grained generator of modular transport: a complicated and non-perturbative operator. It has a simple semi-classical bulk interpretation, however, in terms of a non-local generator that acts on both intervals. The challenge of constructing the fine-grained generator is the same challenge hindering an observer who tries to verify that the Hawking radiation of an evaporating black hole follows a Page curve. Similarly,

the fine-grained entropy is a difficult observable to measure, but has a straightforward interpretation in the semi-classical theory.

Away from a special OPE limit, the QEMC is non-local in the presence of an island and this reflects the non-local nature of modular flow of disjoint intervals. This is most easily seen in X -space where the non-local contributions in (3.62) and (3.66) show up as a coupling between two species of fermions, Ψ_1 and Ψ_2 .

The QEMC therefore has radically different behavior with or without the contribution of an island. An observer in the bath region could start with a (small) interval whose entanglement wedge does not include an island and obtain a local curvature. Increasing the size of the interval, at some point an island will contribute and the QEMC suddenly becomes non-local. We note that this situation bears resemblance to the suggested breakdown of semi-classical physics in the presence of islands [27, 28] and it would be interesting to understand if islands are an avatar for a breakdown of EFT more generally.

One possible way to explore the non-local aspects of the QEMC is by considering the role of the additional contributing zero modes within the framework of von Neumann algebras. Ref. [45] considered the implications of a non-modular geometric phases for the algebra type (especially regards to the existence of a trace functional), and the reformulation of modular Berry transport in the language of von Neumann algebras will be explored in [46]. Perhaps this language can suggest a semiclassical bulk interpretation for the non-local contributions to the QEMC, along the lines of [47]. Another potential approach is to make use of the relation between modular transport and kinematic space. For single intervals in a holographic CFT, the modular curvature equals the Riemann curvature of kinematic space. Defining kinematic space in the presence of a QES, something considered in [48], can perhaps be instructive to better understand the QEMC.

Finally, although we only explicitly studied the QEMC for one JT gravity model on an AdS_2 background, our approach generalizes to non-AdS spacetimes as well. The assumption of our computation was the JLMS relation and did not necessarily require AdS holography. One particular interesting application would be to study modular transport in de Sitter space, similar to studies of the entanglement entropy in cosmological spacetimes [49–64].

Acknowledgements

It is a pleasure to thank Jan de Boer, Bowen Chen, Bartłomiej Czech, Ricardo Espíndola, Jeremy van der Heijden, Bahman Najian and Ronak Soni for helpful discussions. We'd like to thank the Walter Burke Institute for Theoretical Physics at Caltech for hospi-

tality while parts of this work were completed. CZ would also like to thank Arizona State University for hospitality during a semester leave. LA and CK are supported by the Heising-Simons Foundation under the ‘‘Observational Signatures of Quantum Gravity’’ collaboration grant 2021-2818, and CZ acknowledges a Heising-Simons Fellowship as part of this collaboration. CK is also supported by the U.S. Department of Energy under grant number DE-SC0019470. CZ is supported by a UMD Higholt Professorship.

A Riemann Curvature from Fermi Normal Coordinates

In this Appendix, we show how for modular Hamiltonians that reduce to boost Killing vectors only near the edge of the entanglement wedge we can use Fermi normal coordinates to obtain the Riemann curvature from the modular curvature. For simplicity we focus on three dimensions, the higher-dimensional case is also discussed in [14]. We essentially follow their discussion, but specified to the three-dimensional case.

A.1 General Procedure

We consider a spacetime described by Fermi normal coordinates $X^\mu = (X^A, Y)$, where Y is the direction along the geodesic. The metric is given by

$$\begin{aligned} g_{AB} &= \eta_{AB} - \frac{1}{3}R_{ACBD}X^CX^D + \mathcal{O}(X^3) . \\ g_{AY} &= \frac{2}{3}R_{YBCA}X^BX^C + \mathcal{O}(X^3) , \\ g_{YY} &= 1 - R_{YAYB}X^AX^B + \mathcal{O}(X^3) . \end{aligned} \tag{A.1}$$

The modular Hamiltonian is an approximate boost Killing vector near the edge of the entanglement wedge. Using lightcone coordinates $X^\pm = X^0 \pm X^1$ we can write this vector as

$$\zeta = X^+\partial_+ - X^-\partial_- + \mathcal{O}(X^2) . \tag{A.2}$$

Now consider a generator of modular transport V_λ . In the main body, we saw that it can be expressed as

$$V_\lambda = [K'_\lambda, K] , \tag{A.3}$$

where $K = 2\pi\zeta$ and K'_λ is $1/(2\pi)^2$ times the change in the modular Hamiltonian, defined analogously to (3.38). Since K and K'_λ are both (approximate) Killing vectors,

so is V_λ . This implies that it should approximately solve Killing's equation. Dropping the λ subscript to ease notation:

$$g_{\nu\rho}\nabla_\mu V^\rho + g_{\mu\rho}\nabla_\nu V^\rho = \mathcal{O}(X) . \quad (\text{A.4})$$

Denoting the location of the new extremal surface by $X'^A(Y) = 0$, in Fermi normal coordinates this is solved by

$$\begin{aligned} V^A &= X'^A(Y) + \mathcal{O}(X^2) , \\ V^Y &= -\eta_{AB}(\partial_Y X'^A(Y))X^B + \mathcal{O}(X^2) . \end{aligned} \quad (\text{A.5})$$

We now split the generator as $V = V_{(+)} + V_{(-)}$:

$$\begin{aligned} V_{(+)} &= X'^+(Y)\partial_+ + \frac{1}{2}X^-(\partial_Y X'^+(Y))\partial_Y + \mathcal{O}(X^2) , \\ V_{(-)} &= X'^-(Y)\partial_- + \frac{1}{2}X^+(\partial_Y X'^-(Y))\partial_Y + \mathcal{O}(X^2) . \end{aligned} \quad (\text{A.6})$$

With the expansion of the generators of modular transport the modular curvature is given by

$$\mathcal{R}_{+-} = [V_{(+)}, V_{(-)}] . \quad (\text{A.7})$$

However, acting with either $V_{(+)}$ or $V_{(-)}$ changes the location of the extremal surface and therefore changes the Fermi normal coordinate gauge in which the derived expressions for $V_{(+)}$ and $V_{(-)}$ are valid. As explained in [14], we can correct for this by adjusting the $\mathcal{O}(X^2)$ terms to preserve the gauge after acting with one of the generators. This results in

$$\begin{aligned} V^A &= X'^A(Y) + \frac{1}{3}X'^C(Y)\eta^{AD}R_{B(CD)E}X^B X^E , \\ V^Y &= -\eta_{AB}(\partial_Y X'^A(Y))X^B - \frac{1}{3}X'^B(Y)R^Y_{ABC}X^A X^C . \end{aligned} \quad (\text{A.8})$$

We then find¹¹

$$\mathcal{R}_{+-} = [V_{(+)}, V_{(-)}] = \frac{1}{3}X'^+X'^-R_{+-}{}^\mu{}_A X^A \partial_\mu - \frac{1}{2}(\partial_Y X'^-)(\partial_Y X'^+)(X^+\partial_+ - X^-\partial_-) . \quad (\text{A.9})$$

Thus, we explicitly see how the modular curvature is related to the Riemann curvature.

A.2 Example: Diagonal Geodesic in AdS₃

We start from the AdS₃ metric in global coordinates:

$$ds^2 = \ell^2(-\cosh^2 \rho d\tau^2 + d\rho^2 + \sinh^2 \rho d\theta^2) . \quad (\text{A.10})$$

¹¹This corrects a factor of 1/3 absent in (3.20) of [14].

We want to construct Fermi normal coordinates along the diagonal geodesic with endpoints $\tau = 0$ and $\theta = [0, \pi]$. For this purpose, it is useful to first consider Poincaré coordinates which are naturally adapted to this geodesic:

$$ds^2 = \frac{\ell^2}{y^2}(-dt^2 + dx^2 + dy^2) , \quad (\text{A.11})$$

where we define the coordinate system in such a way that the diagonal geodesic is parametrized by $(t, x, y) = (0, 0, y(q))$, where q parametrizes the geodesic. The explicit relation between these coordinates is

$$\begin{aligned} t &= \frac{\ell \cosh \rho \sin \tau}{\cosh \rho \cos \tau - \sinh \rho \sin \theta} , \\ x &= \frac{\ell \sinh \rho \cos \theta}{\cosh \rho \cos \tau - \sinh \rho \sin \theta} , \\ y &= \frac{\ell}{\cosh \rho \cos \tau - \sinh \rho \sin \theta} . \end{aligned} \quad (\text{A.12})$$

The explicit coordinate transformation to Fermi normal coordinates (T, X, Y) is now given by:

$$\begin{aligned} t &= e^{-Y/\ell} T \left(1 + \frac{T^2 - X^2}{3\ell^2} \right) , \\ x &= e^{-Y/\ell} X \left(1 + \frac{T^2 - X^2}{3\ell^2} \right) , \\ y &= e^{-Y/\ell} \ell \left(1 + \frac{T^2 - X^2}{2\ell^2} \right) . \end{aligned} \quad (\text{A.13})$$

The geodesic is described by $(T, X, Y) = (0, 0, Y(q))$. Expanding the metric up to second order in (T, X) away from the geodesic we find

$$ds^2 = - \left(1 + \frac{X^2}{3\ell^2} \right) dT^2 + \left(1 - \frac{T^2}{3\ell^2} \right) dX^2 + \left(1 - \frac{T^2 - X^2}{\ell^2} \right) dY^2 + \frac{2TX}{3\ell^2} dT dX . \quad (\text{A.14})$$

This indeed takes the form of Fermi normal coordinates. Denoting $X^A = (T, X)$ we have

$$\begin{aligned} g_{YY} &= 1 - R_{YAYB} X^A X^B + \mathcal{O}(X^3) , \\ g_{YA} &= -\frac{2}{3} R_{YBAC} X^B X^C + \mathcal{O}(X^3) , \\ g_{AB} &= \eta_{AB} - \frac{1}{3} R_{ACBD} X^C X^D + \mathcal{O}(X^3) . \end{aligned} \quad (\text{A.15})$$

We now have to consider a particular deformation of the diagonal geodesic. We choose to consider a rotation in global coordinates, given by $V = \partial_\theta$. It is easy to compute

that in Fermi normal coordinates, such a rotation corresponds to the following location of the new extremal surface in terms of the $X^\pm = T \pm X$ coordinates:

$$X'^{\pm}(Y) = \pm \ell \sinh(Y/\ell) . \quad (\text{A.16})$$

Evaluating the Riemann components in Fermi normal coordinates we find that up to $\mathcal{O}(X^2)$ the generators are given by

$$\begin{aligned} V_{(+)} &= +\ell \sinh(Y/\ell) \left(1 - \frac{X^+(X^+ + X^-)}{6\ell^2} \right) \partial_+ + \frac{X^-}{2} \cosh(Y/\ell) \partial_Y , \\ V_{(-)} &= -\ell \sinh(Y/\ell) \left(1 - \frac{X^-(X^+ + X^-)}{6\ell^2} \right) \partial_- - \frac{X^+}{2} \cosh(Y/\ell) \partial_Y . \end{aligned} \quad (\text{A.17})$$

Computing the commutator we find

$$\mathcal{R}_{+-} = \frac{X^+}{6} (2 + \cosh(2Y/\ell)) \partial_+ - \frac{X^-}{6} (2 + \cosh(2Y/\ell)) \partial_- . \quad (\text{A.18})$$

This indeed matches the general expression (A.9) when evaluated on the metric (A.14).

B Generators of Modular Transport

Here we write down the generators of modular transport both in x -space as well as in X -space as derived in [26].

B.1 Generators in x -space

For a set of two disjoint intervals described by $[a_1, b_1] \cup [a_2, b_2]$ the generators of modular transport are given by¹²

$$\begin{aligned} V_{a_i} &= \\ &\int dx \frac{\Pi_b^2(x)}{\Delta(x)^2} \left(-\frac{\Pi_a^2(x)}{(a_i - x)^2} T(x) - \frac{\xi \Pi_a(x)}{\Pi_b(a_i) \gamma(x)} \tilde{T}(x) + \frac{\xi(\Delta(x) - \frac{2\Pi_b(a_i)\Pi_a(x)}{(a_i-x)})}{2\Pi_b(a_i)\gamma(x)^2} \psi^\dagger(x) \psi(\tilde{x}) \right) , \\ V_{b_i} &= \\ &\int dx \frac{\Pi_a^2(x)}{\Delta(x)^2} \left(-\frac{\Pi_b^2(x)}{(b_i - x)^2} T(x) + \frac{\xi \Pi_b(x)}{\Pi_a(b_i) \gamma(x)} \tilde{T}(x) - \frac{\xi(\Delta(x) - \frac{2\Pi_a(b_i)\Pi_b(x)}{(b_i-x)})}{2\Pi_a(b_i)\gamma(x)^2} \psi^\dagger(x) \psi(\tilde{x}) \right) . \end{aligned} \quad (\text{B.1})$$

¹²As in the main body, we focus on the + component and drop the explicit + superscripts. We note that our definition of the generators differs from [26] by a minus sign, i.e. $V_\lambda^{\text{us}} = -V_\lambda^{\text{them}}$.

The operator \tilde{T} and coefficients are defined as

$$\tilde{T}(x) = \frac{1}{2} \left(\partial_x \psi^\dagger(x) \psi(\tilde{x}) - (\partial_x \tilde{x}) \psi^\dagger(x) \tilde{\partial}_x \psi(\tilde{x}) \right) , \quad (\text{B.2})$$

and

$$\begin{aligned} \Delta(x) &= (b_1 + b_2 - a_1 - a_2)x^2 + 2(a_1 a_2 - b_1 b_2)x + (a_1 + a_2)b_1 b_2 - (b_1 + b_2)a_1 a_2 , \\ \gamma(x) &= (b_1 + b_2 - a_1 - a_2)x + a_1 a_2 - b_1 b_2 , \\ \Pi_a(x) &= (a_1 - x)(a_2 - x) , \\ \Pi_b(x) &= (b_1 - x)(b_2 - x) , \\ \xi &= -(b_1 - a_1)(b_1 - a_2)(b_2 - a_1)(b_2 - a_2) . \end{aligned} \quad (\text{B.3})$$

The generators obey

$$[V_{a_i}, H] = \partial_{a_i} H , \quad [V_{b_i}, H] = \partial_{b_i} H . \quad (\text{B.4})$$

B.2 Generators in X -space

In X -space the four generators $V_{\lambda=(a_1, a_2, b_1, b_2)}$ can be compactly written as

$$V_\lambda = \int dX \sum_{ij} A_{ij}^{(\lambda)}(X) T_{ij}(X) . \quad (\text{B.5})$$

Defining

$$\tau_{a_1} = \frac{(b_1 - a_2)(b_2 - a_2)}{(b_1 - a_1)(b_2 - a_1)} , \quad \tau_{b_1} = \frac{(b_2 - a_1)(b_2 - a_2)}{(b_1 - a_1)(b_1 - a_2)} , \quad (\text{B.6})$$

the coefficients are given by the four matrices

$$A_{ij}^{(a_1)} = \begin{pmatrix} \frac{b_2 - a_2}{(b_2 - b_1)(b_2 - a_1)} & -\frac{\sqrt{-\tau_{a_1}}}{b_2 - b_1} \\ -\frac{\sqrt{-\tau_{a_1}}}{b_2 - b_1} & \frac{b_1 - a_2}{(b_1 - b_2)(b_1 - a_1)} \end{pmatrix} , \quad A_{ij}^{(a_2)} = \begin{pmatrix} \frac{b_2 - a_1}{(b_2 - a_2)(b_2 - b_1)} & -\frac{\sqrt{-\tau_{a_2}}}{b_1 - b_2} \\ -\frac{\sqrt{-\tau_{a_2}}}{b_1 - b_2} & \frac{b_1 - a_1}{(b_1 - b_2)(b_1 - a_2)} \end{pmatrix} , \quad (\text{B.7})$$

and

$$A_{ij}^{(b_1)} = \begin{pmatrix} 0 & 0 \\ 0 & -\frac{(b_1 - b_2)}{(b_1 - a_1)(b_1 - a_2)} X^2 \end{pmatrix} , \quad A_{ij}^{(b_2)} = \begin{pmatrix} -\frac{(b_2 - b_1)}{(b_2 - a_1)(b_2 - a_2)} X^2 & 0 \\ 0 & 0 \end{pmatrix} . \quad (\text{B.8})$$

References

- [1] S. Ryu and T. Takayanagi, ‘‘Holographic derivation of entanglement entropy from AdS/CFT,’’ *Phys. Rev. Lett.* **96** (2006) 181602, [arXiv:hep-th/0603001](#).

- [2] V. E. Hubeny, M. Rangamani, and T. Takayanagi, “A Covariant holographic entanglement entropy proposal,” *JHEP* **07** (2007) 062, [arXiv:0705.0016 \[hep-th\]](#).
- [3] B. Czech, L. Lamprou, S. Mccandlish, and J. Sully, “Modular Berry Connection for Entangled Subregions in AdS/CFT,” *Phys. Rev. Lett.* **120** no. 9, (2018) 091601, [arXiv:1712.07123 \[hep-th\]](#).
- [4] B. Czech, J. De Boer, D. Ge, and L. Lamprou, “A modular sewing kit for entanglement wedges,” *JHEP* **11** (2019) 094, [arXiv:1903.04493 \[hep-th\]](#).
- [5] B. Czech, L. Lamprou, S. McCandlish, and J. Sully, “Integral Geometry and Holography,” *JHEP* **10** (2015) 175, [arXiv:1505.05515 \[hep-th\]](#).
- [6] J. de Boer, M. P. Heller, R. C. Myers, and Y. Neiman, “Holographic de Sitter Geometry from Entanglement in Conformal Field Theory,” *Phys. Rev. Lett.* **116** no. 6, (2016) 061602, [arXiv:1509.00113 \[hep-th\]](#).
- [7] B. Czech, L. Lamprou, S. McCandlish, B. Mosk, and J. Sully, “A Stereoscopic Look into the Bulk,” *JHEP* **07** (2016) 129, [arXiv:1604.03110 \[hep-th\]](#).
- [8] J. de Boer, F. M. Haehl, M. P. Heller, and R. C. Myers, “Entanglement, holography and causal diamonds,” *JHEP* **08** (2016) 162, [arXiv:1606.03307 \[hep-th\]](#).
- [9] F. S. Nogueira, S. Banerjee, M. Dorband, R. Meyer, J. v. d. Brink, and J. Erdmenger, “Geometric phases distinguish entangled states in wormhole quantum mechanics,” *Phys. Rev. D* **105** no. 8, (2022) L081903, [arXiv:2109.06190 \[hep-th\]](#).
- [10] S. Banerjee, M. Dorband, J. Erdmenger, R. Meyer, and A.-L. Weigel, “Berry phases, wormholes and factorization in AdS/CFT,” *JHEP* **08** (2022) 162, [arXiv:2202.11717 \[hep-th\]](#).
- [11] N. Bao, C. Cao, S. Fischetti, and C. Keeler, “Towards Bulk Metric Reconstruction from Extremal Area Variations,” *Class. Quant. Grav.* **36** no. 18, (2019) 185002, [arXiv:1904.04834 \[hep-th\]](#).
- [12] N. Engelhardt and G. T. Horowitz, “Towards a Reconstruction of General Bulk Metrics,” *Class. Quant. Grav.* **34** no. 1, (2017) 015004, [arXiv:1605.01070 \[hep-th\]](#).
- [13] N. Engelhardt and G. T. Horowitz, “Recovering the spacetime metric from a holographic dual,” *Adv. Theor. Math. Phys.* **21** (2017) 1635–1653, [arXiv:1612.00391 \[hep-th\]](#).
- [14] J. De Boer and L. Lamprou, “Holographic Order from Modular Chaos,” *JHEP* **06** (2020) 024, [arXiv:1912.02810 \[hep-th\]](#).
- [15] J. de Boer, R. Espíndola, B. Najian, D. Patramanis, J. van der Heijden, and C. Zukowski, “Virasoro entanglement Berry phases,” *JHEP* **03** (2022) 179, [arXiv:2111.05345 \[hep-th\]](#).

- [16] B. Czech, J. de Boer, R. Espíndola, B. Najian, J. van der Heijden, and C. Zukowski, “Changing states in holography: From modular Berry curvature to the bulk symplectic form,” *Phys. Rev. D* **108** no. 6, (2023) 066003, [arXiv:2305.16384 \[hep-th\]](#).
- [17] X. Dong, D. Harlow, and A. C. Wall, “Reconstruction of Bulk Operators within the Entanglement Wedge in Gauge-Gravity Duality,” *Phys. Rev. Lett.* **117** no. 2, (2016) 021601, [arXiv:1601.05416 \[hep-th\]](#).
- [18] V. Balasubramanian, B. D. Chowdhury, B. Czech, and J. de Boer, “Entwinement and the emergence of spacetime,” *JHEP* **01** (2015) 048, [arXiv:1406.5859 \[hep-th\]](#).
- [19] B. Freivogel, R. Jefferson, L. Kabir, B. Mosk, and I.-S. Yang, “Casting Shadows on Holographic Reconstruction,” *Phys. Rev. D* **91** no. 8, (2015) 086013, [arXiv:1412.5175 \[hep-th\]](#).
- [20] N. Engelhardt and S. Fischetti, “Covariant Constraints on Holography,” *Class. Quant. Grav.* **32** no. 19, (2015) 195021, [arXiv:1507.00354 \[hep-th\]](#).
- [21] N. Engelhardt and A. C. Wall, “Quantum Extremal Surfaces: Holographic Entanglement Entropy beyond the Classical Regime,” *JHEP* **01** (2015) 073, [arXiv:1408.3203 \[hep-th\]](#).
- [22] G. Penington, “Entanglement Wedge Reconstruction and the Information Paradox,” *JHEP* **09** (2020) 002, [arXiv:1905.08255 \[hep-th\]](#).
- [23] A. Almheiri, N. Engelhardt, D. Marolf, and H. Maxfield, “The entropy of bulk quantum fields and the entanglement wedge of an evaporating black hole,” *JHEP* **12** (2019) 063, [arXiv:1905.08762 \[hep-th\]](#).
- [24] H. Casini and M. Huerta, “Reduced density matrix and internal dynamics for multicomponent regions,” *Class. Quant. Grav.* **26** (2009) 185005, [arXiv:0903.5284 \[hep-th\]](#).
- [25] Y. Chen, “Pulling Out the Island with Modular Flow,” *JHEP* **03** (2020) 033, [arXiv:1912.02210 \[hep-th\]](#).
- [26] B. Chen, B. Czech, L.-Y. Hung, and G. Wong, “Modular parallel transport of multiple intervals in 1+1-dimensional free fermion theory,” *JHEP* **03** (2023) 147, [arXiv:2211.12545 \[hep-th\]](#).
- [27] R. Bousso and G. Penington, “Islands Far Outside the Horizon,” [arXiv:2312.03078 \[hep-th\]](#).
- [28] T. Banks, P. Draper, and M. Karydas, “Breakdown of Field Theory in Near-Horizon Regions,” [arXiv:2401.03572 \[hep-th\]](#).
- [29] J. J. Bisognano and E. H. Wichmann, “On the Duality Condition for Quantum Fields,” *J. Math. Phys.* **17** (1976) 303–321.

- [30] T. Faulkner and A. Lewkowycz, “Bulk locality from modular flow,” *JHEP* **07** (2017) 151, [arXiv:1704.05464 \[hep-th\]](#).
- [31] S. Balakrishnan and O. Parrikar, “Modular Hamiltonians for Euclidean Path Integral States,” [arXiv:2002.00018 \[hep-th\]](#).
- [32] D. L. Jafferis, A. Lewkowycz, J. Maldacena, and S. J. Suh, “Relative entropy equals bulk relative entropy,” *JHEP* **06** (2016) 004, [arXiv:1512.06431 \[hep-th\]](#).
- [33] A. Almheiri and J. Polchinski, “Models of AdS₂ backreaction and holography,” *JHEP* **11** (2015) 014, [arXiv:1402.6334 \[hep-th\]](#).
- [34] J. Engelsöy, T. G. Mertens, and H. Verlinde, “An investigation of AdS₂ backreaction and holography,” *JHEP* **07** (2016) 139, [arXiv:1606.03438 \[hep-th\]](#).
- [35] S. M. Christensen and S. A. Fulling, “Trace Anomalies and the Hawking Effect,” *Phys. Rev. D* **15** (1977) 2088–2104.
- [36] A. Fabbri and J. Navarro-Salas, *Modeling black hole evaporation*. 2005.
- [37] A. Almheiri, R. Mahajan, and J. Maldacena, “Islands outside the horizon,” [arXiv:1910.11077 \[hep-th\]](#).
- [38] T. Hartman, “Entanglement Entropy at Large Central Charge,” [arXiv:1303.6955 \[hep-th\]](#).
- [39] T. Barrella, X. Dong, S. A. Hartnoll, and V. L. Martin, “Holographic entanglement beyond classical gravity,” *JHEP* **09** (2013) 109, [arXiv:1306.4682 \[hep-th\]](#).
- [40] A. Rolph, “Local measures of entanglement in black holes and CFTs,” *SciPost Phys.* **12** no. 3, (2022) 079, [arXiv:2107.11385 \[hep-th\]](#).
- [41] N. Callebaut and H. Verlinde, “Entanglement Dynamics in 2D CFT with Boundary: Entropic origin of JT gravity and Schwarzsian QM,” *JHEP* **05** (2019) 045, [arXiv:1808.05583 \[hep-th\]](#).
- [42] N. Callebaut, “The gravitational dynamics of kinematic space,” *JHEP* **02** (2019) 153, [arXiv:1808.10431 \[hep-th\]](#).
- [43] J. F. Pedraza, A. Svesko, W. Sybesma, and M. R. Visser, “Semi-classical thermodynamics of quantum extremal surfaces in Jackiw-Teitelboim gravity,” *JHEP* **12** (2021) 134, [arXiv:2107.10358 \[hep-th\]](#).
- [44] G. Wong, “Gluing together Modular flows with free fermions,” *JHEP* **04** (2019) 045, [arXiv:1805.10651 \[hep-th\]](#).
- [45] S. Banerjee, M. Dorband, J. Erdmenger, and A.-L. Weigel, “Geometric phases characterise operator algebras and missing information,” *JHEP* **10** (2023) 026, [arXiv:2306.00055 \[hep-th\]](#).
- [46] J. de Boer, J. van der Heijden, B. Najian, and C. Zukowski. To appear.

- [47] N. Engelhardt and H. Liu, “Algebraic ER=EPR and Complexity Transfer,” [arXiv:2311.04281 \[hep-th\]](#).
- [48] A. Gong, C.-B. Chen, and F.-W. Shu, “Kinematic space for quantum extremal surface,” [arXiv:2305.15885 \[hep-th\]](#).
- [49] Y. Chen, V. Gorbenko, and J. Maldacena, “Bra-ket wormholes in gravitationally prepared states,” *JHEP* **02** (2021) 009, [arXiv:2007.16091 \[hep-th\]](#).
- [50] T. Hartman, Y. Jiang, and E. Shaghoulian, “Islands in cosmology,” *JHEP* **11** (2020) 111, [arXiv:2008.01022 \[hep-th\]](#).
- [51] W. Sybesma, “Pure de Sitter space and the island moving back in time,” *Class. Quant. Grav.* **38** no. 14, (2021) 145012, [arXiv:2008.07994 \[hep-th\]](#).
- [52] V. Balasubramanian, A. Kar, and T. Ugajin, “Islands in de Sitter space,” *JHEP* **02** (2021) 072, [arXiv:2008.05275 \[hep-th\]](#).
- [53] H. Geng, Y. Nomura, and H.-Y. Sun, “Information paradox and its resolution in de Sitter holography,” *Phys. Rev. D* **103** no. 12, (2021) 126004, [arXiv:2103.07477 \[hep-th\]](#).
- [54] L. Aalsma and W. Sybesma, “The Price of Curiosity: Information Recovery in de Sitter Space,” *JHEP* **05** (2021) 291, [arXiv:2104.00006 \[hep-th\]](#).
- [55] S. E. Aguilar-Gutierrez, A. Chatwin-Davies, T. Hertog, N. Pinzani-Fokeeva, and B. Robinson, “Islands in Multiverse Models,” *JHEP* **11** (2021) 212, [arXiv:2108.01278 \[hep-th\]](#). [Addendum: *JHEP* 05, 137 (2022), Erratum: *JHEP* 05, 082 (2022)].
- [56] K. Langhoff, C. Murdia, and Y. Nomura, “Multiverse in an inverted island,” *Phys. Rev. D* **104** no. 8, (2021) 086007, [arXiv:2106.05271 \[hep-th\]](#).
- [57] J. Kames-King, E. M. H. Verheijden, and E. P. Verlinde, “No Page curves for the de Sitter horizon,” *JHEP* **03** (2022) 040, [arXiv:2108.09318 \[hep-th\]](#).
- [58] R. Bousso and E. Wildenhain, “Islands in closed and open universes,” *Phys. Rev. D* **105** no. 8, (2022) 086012, [arXiv:2202.05278 \[hep-th\]](#).
- [59] R. Espíndola, B. Najian, and D. Nikolakopoulou, “Islands in FRW Cosmologies,” [arXiv:2203.04433 \[hep-th\]](#).
- [60] A. Svesko, E. Verheijden, E. P. Verlinde, and M. R. Visser, “Quasi-local energy and microcanonical entropy in two-dimensional nearly de Sitter gravity,” *JHEP* **08** (2022) 075, [arXiv:2203.00700 \[hep-th\]](#).
- [61] A. Levine and E. Shaghoulian, “Encoding beyond cosmological horizons in de Sitter JT gravity,” *JHEP* **02** (2023) 179, [arXiv:2204.08503 \[hep-th\]](#).
- [62] S. Azarnia and R. Fareghbal, “Islands in Kerr–de Sitter spacetime and their flat limit,” *Phys. Rev. D* **106** no. 2, (2022) 026012, [arXiv:2204.08488 \[hep-th\]](#).

- [63] K. Goswami and K. Narayan, “Small Schwarzschild de Sitter black holes, quantum extremal surfaces and islands,” *JHEP* **10** (2022) 031, [arXiv:2207.10724 \[hep-th\]](#).
- [64] L. Aalsma, S. E. Aguilar-Gutierrez, and W. Sybesma, “An outsider’s perspective on information recovery in de Sitter space,” *JHEP* **01** (2023) 129, [arXiv:2210.12176 \[hep-th\]](#).